

IN-HOUSE SYMPOSIUM 2016



**DEPARTMENT OF PHYSICS
INDIAN INSTITUTE OF SCIENCE
BANGALORE-560012**

FOREWORD

As a periodic review of its activities, the Department of Physics has been organizing In-house Symposium on annual basis during recent years. This one-day symposium usually consists of oral presentations by faculty members, post-docs and students, and poster presentations by all those who would like to present their recent results. This year we have a total of 20 talks and 55 posters. I hope this package would be a reasonable representation of the ongoing research activities in the department. This event is also particularly useful to freshers (including senior undergraduates) to familiarize themselves with the current research activity in our Department in various branches of Physics.

I would like to thank Manish Jain, Prabal Maiti, Ramesh Mallik, and Nirupam Roy of our department who have shouldered the responsibility to organize this In-house Symposium. I urge all of you to actively participate in this important scientific activity. I hope you will all have an enjoyable and fruitful day.

Prof. V. Venkataraman

Chairman

November 18, 2016

Department of Physics, IISc Bangalore
Inhouse Symposium 2016
November 18, 2016
Auditorium, New Physical Sciences Building

Programme

Session I 9:00-10:30 Chair: Anindya Das

T01	9:00-9:15 K. S. R. Koteswara Rao Shock wave dispersed nano beam epitaxy
T02	9:15-9:30 P. Karnatak Large contact noise in graphene field-effect transistors
T03	9:30-9:45 K. C. Sarkar Fermi Bubbles as signatures of a star-formation driven outflow in our Galaxy
T04	9:45-10:00 D. Prasad AGN jets driven stochastic cold accretion in cluster cores
T05	10:00-10:15 H. Kakoty Role of Entropy in Self Purification of Colloidal Clusters Under Optical Trap
T06	10:15-10:30 H. Ravi Finding number density of caesium by studying the transmission spectrum

10:30-11:00 Tea Break

Session II 11:00-1:00 Chair: Prabal Maiti

T07	11:00-11:15 P. Sharma Curvature Instabilities in Colloidal Membranes
T08	11:15-11:30 A. Agarwala Topological Insulators sans lattices
T09	11:30-11:45 T. Chakraborty Magnetic and electric characterization of organometallic compound $[(\text{CH}_3)_2 \text{NH}_2] \text{Mn}_{0.5} \text{Ni}_{0.5} (\text{HCOO})_3$
T10	11:45-12:00 S. S. N. Chari Nonequilibrium work distribution for force induced melting of a short B-DNA
T11	12:00-12:15 K. Majhi Emergence of a weak topological insulator from the Bi_xSe_y family and the observation of weak anti-localization
T12	12:15-12:30 S. Bag Dramatic changes in DNA conductance with stretching: Structural polymorphism at a critical extension
T13	12:30-12:45 S. Mondal Electronic Band Structure Engineering of Solution Processed Aluminium Oxide Phosphate
T14	12:45-1:00 S. Chakravorty Magneto centrifugal winds from accretion discs around black hole binaries

1:00-2:00 Lunch Break

Session III 2:00-4:30 Poster Session

Session IV 4:30-5:30 Chair: Prateek Sharma

T15 4:30-4:45 N. Roy
 Radio Observations of Galactic Novae: Insights and Surprises

T16 4:45-5:00 G. Prakash
 Anomalous Temperature dependence of electronic and
 Vibrational properties in topological insulator $Sb_2 Te_3$:
 Ultrafast time resolved pump probe study

T17 5:00-5:15 D. Pramanik
 Dendrimer assisted dispersion of carbon nanotubes: a
 molecular dynamics study

T18 5:15-5:30 C. K. Rasmi
 Limited-view light sheet fluorescence microscopy for three
 dimensional volume imaging

T19 5:30-5:45 Roobala
 Evidence of Nanoscale dynamical domains in model binary lipid
 bilayers

 5:45-6:15 High Tea

Session V 6:15-7:15 Chair: V. Venkataraman

Anil Kumar 6:15-7:15 Pratap Raychaudhuri, TIFR, Mumbai
Memorial
Lecture

Berezinski-Kosterlitz-Thouless transition in thin
Superconductin Films

7:15-7:45 Best Poster Award
Viswamitra Memorial Prize
Best write-up Award PH300 (Seminar Course)
Concluding Remarks
7:45-9:00 Dinner

P01	Exploding and Imaging Bubbles in Superfluid Helium	Neha Yadav
P02	Factors influencing the PVC-triggering ability of a cluster of early after depolarization-capable myocytes: A computational study	Soling Zimik
P03	Coherent population trapping (CPT) versus electromagnetically induced transparency (EIT)	Sumanta Khan
P04	Field emission properties and strong localization effect in conduction mechanism of nanostructured perovskite LaNiO_3	Ramesh B. Kamble
P05	Phase transitions in organic crystal Di-isopropyl-ammonium Iodide	Ravi Saripalli
P06	Raman study of pressure induced phase transitions in SnTe	Sukanya Pal
P07	Understanding Dendrimer-Graphene Composite for Supercapacitor Application	Mounika Gosika
P08	A theoretical study of the build-up of the Sun's polar magnetic field by using a 3D kinematic dynamo model	Gopal Hazra
P09	The Tenfold Way: A Group Cohomological View	Vijay B. Shenoy
P10	Direct evidence of tunable 1d superlattice in graphene probed by Magneto-capacitance measurements	Manabendra Kuri
P11	Probing in-plane anisotropy in 2D ReS_2 flakes using conductance and low frequency noise measurement	Richa Mitra
P12	Probing Photo-Induced Conductivity in Bismuth Telluride Nanowires Using Time Resolved Optical Pump Terahertz Probe Spectroscopy	Mithun K. P.
P13	Dendrimers as nanoscale blockers for the toxin cytolysin A (ClyA) protein pores	Subbarao Kanchi
P14	Structure, Micrograph and Transport Properties of Bi_2Te_3 added CoSb_3	Sanyukta Ghosh
P15	Novel photo-tunable transfer characteristics in MoTe_2 - MoS_2 vertical hetero-structure	Arup Kumar Paul
P16	Understanding DNA Based Nanostructures using Molecular Simulations	Himanshu Joshi
P17	Semiconducting Conjugated Microporous Polymer, Poly(1,3,5 triethynylbenzene): Photoelectrochemical Water Splitting, Oxygen Reduction and Supercapacitors	Jayanthi Swetha
P18	Statistical Properties of Inertial-Particle Trajectories in 3D Homogeneous and Isotropic Super-fluid Turbulence	Akhilesh Kumar Verma
P19	Observation of Andreev reflection at the junction of graphene quantum Hall state and superconductor	Manas Ranjan Sahu
P20	Temperature Dependent Charge Transport Study in Hybrid Composite Devices of Organic Semiconductor and Quantum Dots	Motiur Rahman Khan
P21	Raman Spectroscopic Studies on Bismuth Doped $\text{Eu}_2\text{Ir}_2\text{O}_7$	Anoop Thomas
P22	Electrical switching, local structure and thermal crystallization in Al-Te glasses	Pumlianmunga
P23	Shear induced 3D ordering and instabilities in Surfactant Mesh Phases: Coupling between flow and membrane defects	Pradip Kumar Bera
P24	Magnetic field assisted magnetization reversal in permalloy nanoringnanowire structures	Manohar Lal
P25	Glassy dynamics in dense assembly of active dumbbells	Rituparno Mandal
P26	Thermal conductivity of glass-forming liquids	Pranam Jyoti Bhuyan

P27	Spin liquid like Raman signatures in hyperkagome iridate $\text{Na}_4\text{Ir}_3\text{O}_8$	Satyendra Nath Gupta
P28	A micrometre-sized heat engine operating between bacterial reservoirs	Sudeesh Krishnamurthy
P29	Growth defects causing anomalous magnetic behaviour and unusual exchange bias with vertically shifted magnetic hysteresis loop in a pure antiferromagnetic system	Tanushree Sarkar
P30	Quasiparticle band structure and optical properties of hexagonal- YMnO_3	Tathagata Biswas
P31	Origin of layer dependence in band structures of two-dimensional materials	Mit Naik
P32	Electron Phonon coupling measurement in top gated atomically thin ReS_2 transistor	Subhadip Das
P33	Origin of 1/f Noise in MBE grown ferromagnetically doped and undoped Topological Insulators	Saurav Islam
P34	Size and layer dependence of thermally induced ripples in h-BN sheets	Indrajit Maity
P35	Statistics of Trajectories and Geometry of Light Inertial Particles in Turbulence	P. Shubham Parashar
P36	Emergent Topological order from Spin-Orbit Density wave	Gaurav Gupta
P37	Electrical transport and low frequency 1/f noise study in the hybrid of molybdenum disulphide and SrTiO_3	Anindita Sahoo
P38	Multiferroic properties of hexagonal LuFeO_3 nanoparticles	Pittala Suresh
P39	Coherent mixing and control dephasing of quantum hall edge states in graphene p-n-p/n-p-n device	Chandan Kumar
P40	Accessing Rashba states in electrostatically gated topological insulator devices	Abhishek Banerjee
P41	Light induced carrier transport across Van der Waals heterostructure: WSe_2 -graphene	Jayanta Kumar Mishra
P42	^{23}Na , ^{29}Si MAS NMR investigation of $\text{Sr}_{1-x}\text{Na}_x\text{SiO}_{3-0.5x}$ ($x=0.45$) fast ion conductor	P. Lokeswara Rao
P43	Anomalous superconductivity in delta-doped semiconductors near the Mott transition	Saquib Shamim
P44	Non-Boltzmann thermoelectricity at a single Van der Waal junction	Phanibhusan Singhamahapatra
P45	Microscopic Origin of Electron Traps in Chemical Vapour Deposition grown Monolayer MoS_2 and its Grain Boundaries	Kimberly Hsieh
P46	Carrier Dynamic in Twisted Bilayer Graphene Probed by Time Resolved Terahertz Spectroscopy	Srabani Kar
P47	Log-normal electron localization in strongly gapped bilayer graphene	M. A. Aamir
P48	Direct Measurement of Growing Interfacial Tension of Spatially Correlated Regions on Approaching the Colloidal Glass Transition	Divya Ganapathi
P49	Experiments on atomic-scale point contacts in graphene	Amogh Kinikar
P50	Number-resolving single photon detector from band-engineered van der Waals heterostructures	Kallol Roy
P51	Transverse Thermoelectric response and Diamagnetism as a probe of superconducting fluctuation, vortex-Nernst-boundary in quasi-2D High T_c superconductors	Kingshuk Sarkar
P52	Unconventional Phases of Attractive Fermi Gases in Synthetic Hall Ribbons	Sudeep Kumar Ghosh
P53	\mathcal{PT} -Symmetric Non-Hermitian Superconductor	Ananya Ghatak

TALK ABSTRACTS

Shock wave dispersed nano beam epitaxy

K. S. R. Koteswara Rao, Atul Abhale and K. P. J. Reddy^{a)}

Department of Physics, ^{a)}Aerospace Engineering, I. I. Sc., Bangalore, INDIA

Email: ksrkrao@physics.iisc.ernet.in

Abstract

In this abstract, we introduce a new technique called "shock wave dispersed nano beam epitaxy (SD-NBE)" to create nano-layers of quantum dots towards development of ultra-thin-film devices. Though the technique is not limited to QDs, any other material in solution form such as conducting or insulating polymers, solution dispersed CNTs, fluorescents, photoresist etc., can be deposited on variety of substrates irrespective of the nature of substrate (silicon, glass, metal, polymer film etc.). It is based on the nano-dispersion technique that exploits the phenomena, which produce focused weak shock waves and disperse nanomaterials. Here, the solution dispersed PbS/CdTe QDs have been deposited on Si, SiO₂/Si substrates and found to have suitable physical, electrical and optical properties to be useful in the development of thin-film devices. This novel technique is inexpensive, economically uses quite a small amount of material and minimizes the wastage; hence, it can be well implemented in various applications of material physics and device technology at nanoscale.

Large contact noise in graphene field-effect transistors

P. Karnataka^{1*}, T.P. Sai^{1*}, S. Goswami^{1*}, S. Ghatak¹, S. Kaushal², A. Ghosh¹

¹Department of Physics, Indian Institute of Science, Bangalore 560 012, India.

²Tokyo Electron Ltd., Akasaka Biz Tower, 3-1 Akasaka 5-Chome, Minato-ku, Tokyo 107-6325, Japan.

paritosh@physics.iisc.ernet.in

Abstract

Intrinsic time-dependent fluctuation in the electrical resistance at the graphene-metal interface, or the contact noise, adversely affects the performance of graphene field effect transistors but remains largely unexplored. In this talk, I will discuss how we exploit varying device geometry and contact configuration, in transistors with channel carrier mobility ranging from $5,000 \text{ cm}^2\text{V}^{-1}\text{s}^{-1}$ to $80,000 \text{ cm}^2\text{V}^{-1}\text{s}^{-1}$, to reliably estimate the contact contribution to the measured device noise. A phenomenological model developed for contact noise due to current crowding for two dimensional conductors, shows that the contacts dominate the measured resistance noise in all graphene field effect transistors when measured in the two-probe or invasive four probe configurations, and surprisingly, also in nearly noninvasive four probe (Hall bar) configuration in the high mobility devices. I will highlight the role of current crowding, discuss the microscopic mechanism of contact noise and possible ways to minimize it. Our results could be generic to two dimensional material-based electronic devices and may lead to ultra-low noise electronics in two dimensional hybrids.

*Equal Contributions.

References

- [1] P. Karnataka, T.P. Sai, S. Goswami, S. Ghatak, S. Kaushal, A. Ghosh, Nature Communications (2016, accepted). arXiv:1611.01181.

Topological Insulators sans lattices

Adhip Agarwala* and Vijay B. Shenoy†

*Centre for Condensed Matter Theory, Department of Physics,
Indian Institute of Science, Bangalore 560 012, India*

(Dated: November 10, 2016)

Abstract

Our understanding of topological insulators is based on an underlying lattice where the local electronic degrees of freedom at different site interact with each other in ways that produce non-trivial band topology. Indeed, the search for material systems to realize such phases have been strongly influenced by this. In this work, we show that topological insulating phases do not need a lattice. We demonstrate this by explicitly constructing models on set of sites randomly distributed in space. By studying the quantized conductances and Bott indices, we systematically show the topological character of the states in such random system in two spatial dimensions in the symmetry classes A, AII, D, DIII and C. We also demonstrate a time reversal invariant topological insulator on a random set of sites in three spatial dimensions. Our study not only provides a deeper understanding of the topological phases of non-interacting electrons, but also suggests new routes of creating them via a random distribution of impurities in an otherwise insulating host.

* adhip@physics.iisc.ernet.in

† shenoy@physics.iisc.ernet.in

AGN jets driven stochastic cold accretion in cluster cores

Deovrat Prasad¹, Prateek Sharma¹ and Arif Babul^{2,3}

November 11, 2016

¹Department of Physics & Joint Astronomy Programme, Indian Institute of Science, Bangalore, India -560012.

²Department of Physics and Astronomy, University of Victoria, Victoria, BC V8P 1A1, Canada

³Institute of Computational Science, Center for Theoretical Astrophysics and Cosmology, University of Zurich, Winterthurerstrasse 190, 8057, Zurich, Switzerland

Abstract

Several arguments suggest that stochastic condensation of cold gas and its accretion onto the central supermassive black hole (SMBH) is essential for active galactic nuclei (AGN) feedback to work in the most massive galaxies that lie at the centers of galaxy clusters. Our $3 - D$ AGN jet-ICM (intracluster medium) simulations show that the angular momentum of the cold gas crossing < 1 kpc is essentially isotropic. With almost equal mass in clockwise and counter-clockwise orientations, we expect a cancellation of angular momentum on roughly the dynamical time. This means that a compact accretion flow with a short viscous time ought to form, through which enough accretion power can be channeled into jet mechanical energy sufficiently quickly to prevent a cooling flow. The inherent stochasticity, expected in feedback cycles driven by cold gas condensation, gives rise to a large variation in the cold gas mass at the centers of galaxy clusters, for similar cluster and SMBH masses, in agreement with the observations. Such correlations are expected to be much tighter for the smoother hot/Bondi accretion. The weak correlation between cavity power and Bondi power obtained from our simulations also match observations.

Role of Entropy in Self Purification of Colloidal Clusters Under Optical Trap

Hreedish Kakoty¹, Rajarshi Banerjee¹, Chandan Dasgupta¹, Ambarish Ghosh^{1,2,3}

¹*Department of Physics, Indian Institute of Science, Bangalore-560012*

²*Department of Electrical Communication Engineering, Indian Institute of Science, Bangalore-560012*

³*Centre for Nano Science and Engineering, Indian Institute of Science, Bangalore-560012*

Controlling the structure of a collection of colloidal particles under external forces can be helpful in developing soft nanomaterials with novel functionalities. How external impurities organize within such confined systems is of fundamental and technological interest, especially when the system sizes are so small that even a single dopant can interact with an appreciable fraction of the system. In spite of multiple techniques available to study colloidal clusters under external confinement, experiments to specifically probe the behaviour of dopants have been relatively few. Here, we have used a defocused laser beam to form colloidal clusters in two dimensions with precise control over the size and phase of the assembly. Crucially, we could inject and subsequently study the behaviour of foreign dopants within these crystallites, which has revealed surprising position dependence in the fate of dopants getting either spontaneously expelled or permanently internalized within the assembly. We have modelled this system numerically and found that this phenomenon arises due to the subtle interplay between the effects of external confinement and role of entropy in the thermodynamics of small assemblies of interacting particles. There is a distant parallel between the phenomena reported here and the self-purification of dopants in solid state nanomaterials, such as Mn atoms in semiconducting nanocrystals [1, 2], although the spatial dependence of the external confining potential plays a major role in the phenomena reported here, which is absent for atomic clusters. The studies presented here could be extended to host colloids of higher degree of complexity [3], e.g. non-spherical shapes, self-propelled particles [4] etc., and the insight gained could be useful in designing and assembling new type of soft nanomaterials having properties of self purification [5, 6].

[1] Steven C Erwin, Lijun Zu, Michael I Hafet, Alexander L Efros, Thomas A Kennedy and David J Norris. Doping semiconductor nanocrystals. *Nature*, 436(7047):91-94, 2005.

[2] Gustavo M Dalpian and James R Chelikowsky. Self-purification in semiconductor nanocrystals. *Physical review letters*, 96(22):226802, 2006.

[3] Hartmut Lowen. Introduction to colloidal dispersions in external fields. *The European Physical Journal Special Topics*, 222(11):2727-2737, 2013.

[4] MC Marchetti, JF Joanny, S Ramaswamy, TB Liverpool, J Prost, Madan Rao and R Aditi Simha. Hydrodynamics of soft active matter. *Reviews of Modern Physics*, 85(3):1143, 2013.

[5] Gi-Ra Yi, David J Pine and Stefano Sacanna. Recent progress on patchy colloids and their self-assembly. *Journal of Physics: Condensed Matter*, 25(19):193101, 2013.

[6] Fan Li, David P Josephson, and Andreas Stein. Colloidal assembly: the road from particles to colloidal molecules and crystals. *Angewandte Chemie International Edition*, 50(2):360-388, 2011.

Finding number density of caesium by studying the transmission spectrum.

Harish Ravi, Mangesh Bhatrai, and Vasant Natarajan

November 8, 2016

Abstract

We study the absorption profile of a vapor of Cs atoms. We extract the number density by fitting this curve to a numerical density-matrix model. We then study the absorption as a function of temperature, and combined with using the Clausius-Clapeyron equation, to estimate the latent heat of evaporation. The asymmetric line-shape of the absorption profile requires the use of a two-region model with and without the presence of the laser beam, something which the package that we use allows.

Title: Curvature Instabilities in Colloidal Membranes

Authors: Lachit Saikia, Meera Thomas, V. A. Raghunathan and Prerna Sharma

Abstract:

Membrane curvature generation and remodeling are critical for trafficking and cellular functions. Local curvature generation is associated mainly with specialized proteins which use mechanisms such as protein crowding, nanoscopic and macroscopic scaffolding. We investigate curvature generation in a highly simplified model system of colloidal membranes and show that structural phase transitions within the membrane alone are enough to result in membrane curvature and wrinkling. We determine the structure and dynamics of the buckled colloidal membranes using a variety of microscopy and scattering techniques to identify the relevant parameters in the phase transition that affect the overall morphology of the membranes

Abstract for Talk in Inhouse symposium - 2017

Title: Fermi Bubbles as signatures of a star-formation driven outflow in our Galaxy

Authors: Kartick C Sarkar (IISc & RRI, JAP), Biman Nath (RRI), Prateek Sharma (IISc)

Abstract: Modelling of emission from multiphase galactic outflows is important to decipher the feedback processes in galaxies. Fermi Bubbles (FBs) are excellent laboratories for such studies as they shine in radio, x-ray, gamma rays and also show kinematic signatures in UV absorption. Using hydrodynamical simulations, we show that these bubbles can arise from a star formation activity at the Galactic Centre with a star formation rate of 0.3-0.5 Msun/yr sustaining over a time scale of ~30 Myrs. By modelling the X-ray emission related to the FBs, we constrain the central halo density in our Galaxy to be $\sim 3e-3$ m_p/cc. Our modelling of radio emission suggests that the magnetic field inside these bubbles is $\sim 3-5$ microG, and is sufficient to give rise to the observed gamma-ray spectrum by inverse Compton scattering of CMB by cosmic rays. Our model also provides explanation of the observed kinematics of absorption lines through the FBs.

Magnetic and electric characterization of organometallic compound [(CH₃)₂NH₂]Mn_{0.5}Ni_{0.5}(HCOO)₃

Tirthankar Chakraborty^{*1}, and Suja Elizabeth¹

¹Department of Physics, Indian Institute of Science, Bangalore-560012, India

* Presenting author: tirtha255@gmail.com

Hybrid frameworks, usually known as metal-organic framework (MOF), are popular due to their potential application in gas storage, nonlinear optics, drug delivery, catalysis and magnetism. The recent observation of multiferroic property in MOFs with order-disorder hydrogen bonding transition has evoked great research interest in these materials. Dimethylammonium metal formate with ABX₃ type topology is a well-studied family in this regard [1,2]. Here, we report magnetic, electric and impedance spectroscopic characterizations of hetero-metallic MOF [(CH₃)₂NH₂]Mn_{0.5}Ni_{0.5}(HCOO)₃ (MnNi-DMF).

MnNi-DMF is prepared via solvothermal method. Phase purity and crystal structure at room temperature are confirmed by powder X-ray diffraction. Isothermal field variation and temperature variation of magnetization indicate antiferromagnetic ordering with weak ferromagnetism. The antiferromagnetic structure results in DM interaction leading to spin canting and “*weak ferromagnetism*”. Thermally activated relaxation observed in dielectric studies is likely to be due to ordering of dimethylamine cation and associated with first order improper antiferroelectric transition. Temperature dependence of polarization is analyzed by measurement of pyroelectric current. Spontaneity of polarization was confirmed with different protocols of pyroelectric current measurement. Electric ordering is clearly reflected in impedance spectroscopic measurements. Two distinct regions can be demarcated above and below the electric ordering temperature based on resistance and capacitance of equivalent circuit model and activation energy. Coexistence of magnetic and electric ordering makes the system multiferroic at low temperature.

References:

- [2] P. Jain, N. S. Dalal, B. H. Toby, H. W. Kroto, and A. K. Cheetham, Journal of the American Chemical Society 130, 10450 (2008)
- [3] P. Jain, V. Ramachandran, R. J. Clark, H. D. Zhou, B. H. Toby, N. S. Dalal, H. W. Kroto, and A. K. Cheetham, Journal of the American Chemical Society 131, 13625 (2009)
- [4] M. Maczka, A. G. agor, B. Macalik, A. Pikul, M. Ptak, and, J. Hanuza, Inorganic chemistry 53, 457 (2014)
- [5] Z. Wang, P. Jain, K.-Y. Choi, J. Van Tol, A. K. Cheetham, H. W. Kroto, H.-J. Koo, H. Zhou, J. Hwang, E. S. Choi, et al., Physical Review B 87, 224406 (2013)

Nonequilibrium work distribution for force induced melting of a short B-DNA

S. Siva Nasarayya Chari and Prabal K. Maiti

Department of Physics, Indian Institute of Science, Bangalore 560012.

Abstract : Since from the discovery of double helical structure of DNA, several studies have been made to understand its molecular properties. Recent advances in nanotechnology made it possible to study the mechanical properties of single biomolecules. In this work, we investigate the force induced melting of a double stranded B-DNA, of specified sequence using atomistic simulation. The 12-mer DNA is restrained at one end (3' and 5') and pulled from the other end by applying force at a constant rate, along its helical axis. The extension(x) of DNA as a function of applied force(F) is obtained and associated (nonequilibrium)work done is estimated by numerically integrating $x(F)$ over the total range of values of F .

The nonequilibrium work distribution is obtained from several such pulling experiments. We then use Jarzynski equality to estimate the free energy difference between the initial unstretched and final over-stretched equilibrium states.

Emergence of a weak topological insulator from the Bi_xSe_y family and the observation of weak anti-localization.

Kunjalata Majhi, Koushik Pal, Himanshu Lohani, Abhishek Banerjee,
Pramita Mishra, Anil K Yadav, R Ganesan, BR Sekhar, Umesh V
Waghmare, and PS Anil Kumar.

The discovery of strong topological insulators led to enormous activity in condensed matter physics and the discovery of new types of topological materials. Bismuth based chalcogenides are exemplary strong three dimensional topological insulators that host an odd number of massless Dirac fermionic states on all surfaces. A departure from this notion is the idea of a weak topological insulator, wherein only certain surface terminations host surface states characterized by an even number of Dirac cones leading to exciting new physics. Experimentally however, weak topological insulators have proven to be elusive. Here, we report the discovery of a weak topological insulator (WTI), BiSe, of the Bi-chalcogenide family with an indirect band gap of 42 meV. Its structural unit consists of bismuth bilayer (Bi_2), a known quantum spin hall insulator sandwiched between two units of Bi_2Se_3 which are three dimensional strong topological insulators. Angle resolved photo-emission spectroscopy (ARPES) measurements on cleaved single crystal flakes along with density functional theory (DFT) calculations confirm the existence of weak topological insulating state of BiSe. Additionally, we have carried out magneto-transport measurements on single crystal flakes as well as thin films of BiSe, which exhibit clear signatures of weak anti-localization at low temperatures, consistent with the properties of topological insulators.

Dramatic changes in DNA conductance with stretching: structural polymorphism at a critical extension

Saiantan Bag

Using multiscale modeling, we study the conductance of dsDNA as it is mechanically stretched to promote various structural polymorphisms. We calculate the current along the stretched DNA using a combination of molecular dynamics simulations, non-equilibrium pulling simulations, quantum mechanics calculations, and kinetic Monte Carlo simulations. For 5'end1-5'end2 attachments we find an abrupt jump in the current within a very short stretching length (6 Å or 17 %) leading to a melted DNA state. In contrast, for 3'end1-3'end2 pulling it takes almost 32 Å(84 %) of stretching to see the similar jump in current. Thus we demonstrate that charge transport in DNA can happen over such large stretching length of several nanometers. We attribute this unexpected behaviour to the B to S conformational DNA transition and highly inclined base pair geometry in this pulling protocol. We find that the dramatically different conductance behaviors for these two pulling protocols arise from the nature of how hydrogen bonds of DNA base pairs break.

Reference: S. Bag, S. Mogurampelly, W. A. Goddard III and P. K. Maiti, *Nanoscale*, 2016, 8, 16044-16052.

Electronic Band Structure Engineering of Solution Processed Aluminium Oxide Phosphate

Sandip Mondal*, V. Venkataraman

Department of Physics, Indian Institute of Science, Bangalore 560012, India

*Email: sandipmondal@physics.iisc.ernet.in / Tel: (0091) 95351 45707

Low cost, sol-gel spin-coated Aluminium Oxide Phosphate (ALPO) is a promising candidate for application as gate insulator in various electronic devices [1]. Due to its transparent nature it also has wide applications in optical devices [2]. Further, ALPO is a considerably excellent dielectric for use as trapping and blocking layer of memory devices because of its wide band gap, low leakage current and modest value of dielectric constant [3]. In spite of the wide optoelectronic applications of ALPO, its entire electronic structure is unknown. Here, we demonstrate an interesting change in electronic band structure of ALPO due to different annealing temperature by using the x-ray photoelectron spectroscopy (XPS) as well as ultra-violet photoelectron Spectroscopy (UPS) measurements.

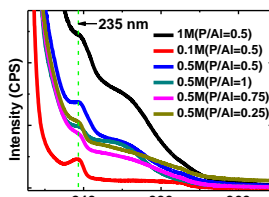


Fig.1 UV-visible spectra of liquid ALPO

Sample Preparation:

- The sol-gel ALPO prepared from literature[4] with different concentrations
- Piranha Cleaned p-Si ($\sim 10^{15} \text{ cm}^{-3}$)
- Exposed to Plasma (0.005 mbar/20 m)
- 90 nm ALPO film deposited by spin coating with P/Al=0.5 (0.5M) & annealed
- Thermally evaporated 200nm aluminium on half of ALPO film
- 5 nm ALPO film etched inside the XPS system with plasma to remove the carbon contamination

The UV-visible spectroscopy of sol-gel ALPO shows a strong absorption peak at 5.3 eV (235 nm) in liquid condition [fig.1], which is quite different from its solid state band gap. In order to find the actual band gap (E_g) of ALPO film, we adopt inelastic energy loss spectra of O 1s of high-k dielectric method [5]. In addition, we use UPS to extract electron affinity (χ). To check the accuracy of these methods, standard thermally grown 50 nm silicon di-oxide has been used. The values of E_g and χ are match well with the literature as shown in fig 2.

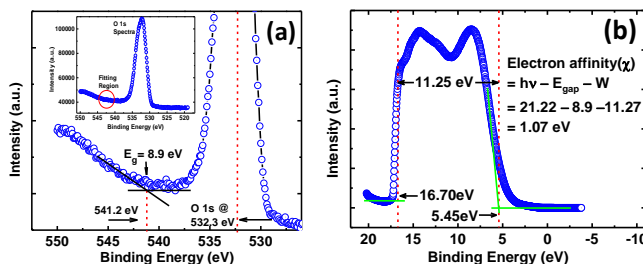


Fig 2 (a) Energy loss spectrum of O1s of SiO_2 film on Si, INSET: O1s peak.; (b) UPS spectrum of SiO_2 with He I

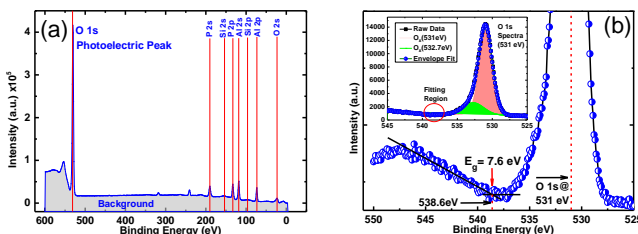


Fig 3. (a) XPS survey for ALPO is showing primary photoelectric peak with substrate Si peak; (b) Energy loss spectrum of O1s of ALPO film on Si, INSET: O1s peak with two oxidation state (531 & 532 eV)

A survey scan using XPS was made using 180 eV pass energy with a step 1eV as shown in fig 3(a). The survey scan is showing all the elements of ALPO as well as substrate peak. There is no carbon contamination found in the sample. The band gap energy is equal to the difference between the core level peak energy and

onset of inelastic losses, $E_g = E_{loss} - E_{O1s} = 540 - 532.4 = 7.6 \text{ eV}$ [Fig. 3(b)].

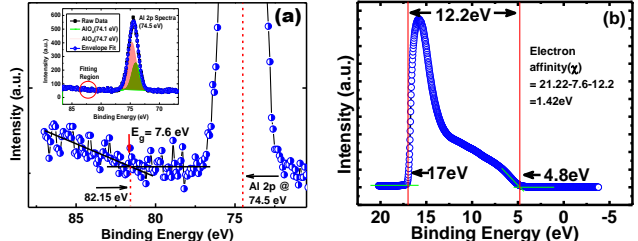


Fig. 4 (a) Energy loss spectrum of Al 2p of ALPO film on Si, INSET: Al 2p peak with oxidation state (74.1 & 74.7 eV); (b) UPS spectrum of ALPO with He I

The E_g is verified with inelastic energy loss spectra of Al 2p peak of ALPO, $E_g = E_{loss} - E_{Al2p} = 82.15 - 74.5 = 7.6 \text{ eV}$ [fig. 4(a)]. The electron affinity (χ_{ALPO}) has been calculated from UPS spectra by using the He I (21.2 eV) source [6]. If W is the total width of the spectra and $h\nu$ is the photon energy source then $\chi = h\nu - E_g - W = 21.22 - 7.6 - 12.27 = 1.35 \text{ eV}$ [fig.4 (b)]. The UPS measurement was done on ALPO films annealed at different temperatures and it was found that there is a systematic decrease in χ_{ALPO} . The schematic entire band structure with the change in χ_{ALPO} is drawn in fig 5.

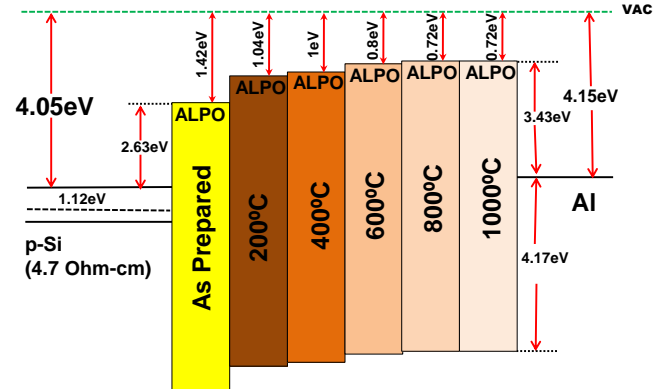


Fig. 5. ALPO band structure on p-Si with Al gate electrode with different processing temperature.

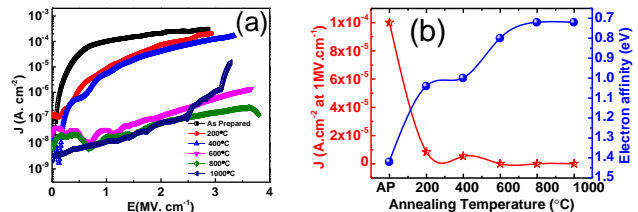


Fig. 6. (a) The leakage current of ALPO processed at different temperature; (b) The change in leakage current with electron affinity due to the variation in annealing temperature.

The consequence of change in χ_{ALPO} is reflected on the leakage current density (J) of the ALPO films as shown in fig 6. Observed maximum leakage current is $1.0 \times 10^{-4} \text{ A.cm}^{-2}$ (at $1\text{MV} \cdot \text{cm}^{-1}$) for the as prepared film and decreases to $1.2 \times 10^{-8} \text{ A.cm}^{-2}$ (at $1\text{MV} \cdot \text{cm}^{-1}$), film annealed at 1000°C . The large change in leakage current is attributed to the change in χ_{ALPO} with film processing temperature.

REFERENCES: [1] APL. 99, 24 (2011); [2] J. Vac. Sci. Technol. B, 28, 6 (2010); [3] IEEE EDL37, 4 (2016); [4] Chem. Mater., 19, 16 (2007); [5] JAP 115, 094105 (2014); [6] PRB, 78, 085114 (2008)

Inhouse Symposium 2016: Abstract for Talk

Title: Magneto centrifugal winds from accretion discs around black hole binaries

Authors: Susmita Chakravorty, Pierre-Olivier Petrucci, Jonathan Ferreira

Abstract:

High resolution X-ray spectra of black hole X-ray binaries (BHBs) show blueshifted absorption lines suggesting the presence of outflowing winds. Furthermore, observations show that the disk winds are equatorial and they occur in the Softer (disk dominated) states of the outburst and are less prominent or absent in the Harder (power-law dominated) states. We are testing if self-similar magneto-hydrodynamic (MHD) accretion-ejection models can explain the observational results for accretion disk winds in BHBs. In our models, the density at the base of the outflow, from the accretion disk, is not a free parameter, but is determined by solving the full set of dynamical MHD equations without neglecting any physical term. Different MHD solutions were generated for different values of (a) the disk aspect ratio and (b) the ejection efficiency ' p '. We generated two kinds of MHD solutions depending on the absence (cold solution) or presence (warm solution) of heating at the disk surface. The cold MHD solutions are found to be inadequate to account for winds due to their low ejection efficiency. The warm solutions can have sufficiently high values of p ($>= 0.1$) which is required to explain the observed physical quantities in the wind. The heating (required at the disk surface for the warm solutions) could come from (i) the dissipation of energy due to MHD turbulence in the disk or (ii) from the illumination of the disk surface which would be more efficient in the Soft state. We found that in the Hard state a range of ionisation parameters is thermodynamically unstable, which makes it impossible to have any wind at all, in the Hard state. Thus, using the MHD outflow models we are able to explain the observed trends, i.e. that the winds are equatorial and that they are observable in the Soft states (and not expected in the Hard state) of the BHB outbursts.

Encouraged by the success of the models we are formalising methods to predict theoretical high resolution spectra to be fitted to absorption line observations from XMM-Newton and Chandra gratings. Our models will include the key physical parameter p (the ejection efficiency) of the accretion disk. Hence we hope to directly constrain physical parameters of the disk by fitting the observed spectra.

Radio Observations of Galactic Novae: Insights and Surprises

Nirupam Roy (ENova Team and GNova group collaborations)

Novae are sudden visual brightening of star triggered by runaway thermonuclear burning on the surface of an accreting white dwarf. Although they are fairly common and bright event, multiple fundamental questions about them, like the discrepancy in observed and theoretical ejecta mass, or their possible connection with supernovae, remain unanswered. Despite their astronomical significance as nearby laboratory for the study of nuclear burning and accretion phenomena, multiple such discrepancies suggest surprising limits to our physical understanding of these events. In this talk, I will describe how radio observations with complementary multiwavelength campaigns can potentially play a crucial role in addressing some of these puzzling issues.

Anomalous Temperature dependence of electronic and vibrational properties in topological insulator Sb_2Te_3 : Ultrafast time resolved pump probe study

Gyan Prakash,¹ Koushik Pal,² Manish Jain,³ U. V. Waghmare,² and A. K. Sood¹

¹*Department of Physics and Center for Ultrafast Laser Applications,
Indian Institute of Science, Bangalore 560012, India*

²*Theoretical Sciences Unit, Jawaharlal Nehru Centre for
Advanced Scientific Research Jakkur campus, Bangalore 560064*

³*Department of Physics, Indian Institute of Science, Bangalore -560012*

Abstract

Sb_2Te_3 is a prototypical example of strong 3D topological insulator with only one Dirac cone in its surface electronic structure. Recent experiments on thermal expansion of Sb_2Te_3 have shown an intriguing anomaly in thermal expansion along the hexagonal axis in the temperature range of 200-250K, with no accompanying signatures in the specific heat. The origin of the anomaly is not known so far. We present femtosecond pump-probe differential reflectivity measurements on single crystals of Sb_2Te_3 at temperatures from 3 to 300K to determine temperature dependence of coherent optical and acoustic phonons along with the carrier dynamics. Our results clearly show anomalous temperature dependence of the parameters associated with vibrational and electronic relaxation in the narrow temperature range of 200-250K. Using first-principles density functional theory (DFT) calculations, we show that the observed temperature dependent anomalies can be explained with a mechanism of formation of energetically favorable stacking faults above 200K. As similar kinds of phenomena are also observed in other chalcogenides in the same crystal family e.g in Bi_2Se_3 and Bi_2Te_3 , the proposed mechanism for Sb_2Te_3 also holds true for these strong topological insulators.

Dendrimer assisted dispersion of carbon nanotubes: a molecular dynamics study

Debabrata Pramanik and Prabal K Maiti

Centre for Condensed Matter Theory, Department of Physics, Indian Institute of Science,
Bangalore 560012, India

Abstract

Various unique physical, chemical, mechanical and electronic properties of carbon nanotube (CNT) make it very useful materials for diverse potential application in many fields. Experimentally synthesized CNTs are generally found in bundle geometry with a mixture of different chirality and present a unique challenge to separate them. In this paper we have proposed the PAMAM dendrimer to be an ideal candidate for this separation. To estimate efficiency of the dendrimer in dispersion of CNTs from the bundle geometry, we have calculated potential of mean forces (PMF). Our PMF study of two dendrimer wrapped CNTs shows lesser binding affinity compared to the two bare CNTs. PMF study shows that the binding affinity decreases for non-protonated dendrimer and for the protonated case, the interaction is fully repulsive in nature. For both the non-protonated as well as protonated cases, the PMF increases with increasing dendrimer generations from 2 to 4 gradually compare to the bare PMF. We have performed PMF calculations with (6,5) and (6,6) chirality to study the chirality dependence of PMF. Our study shows that the PMFs between two (6,5) and two (6,6) CNT's respectively are ~ -29 kcal/mol and ~ -27 kcal/mol. Calculated PMF for protonated dendrimer wrapped chiral CNT's is more compared to the protonated dendrimer wrapped armchair CNTs for all the generations studied. However, for non-protonated dendrimer wrapped CNTs such chirality dependence is not very prominent. Our study suggests that the dispersion efficiency of protonated dendrimer is more compared to the non-protonated dendrimer and can be used as an effective dispersing agent in dispersion of CNT from the bundle geometry.

Reference:

1. D. Pramanik and Prabal K. Maiti, Dendrimer assisted dispersion of carbon nanotubes: a molecular dynamics study, *Soft Matter*, 2016, 12, 8512-8520.

LIMITED-VIEW LIGHT SHEET FLUORESCENCE MICROSCOPY FOR THREE DIMENSIONAL VOLUME IMAGING

C. K. Rasmi^{1,2}, Kavya Mohan¹, M. Madhangi³, K. Rajan², U. Nongthombam³ and Partha P. Mondal¹

¹Nanobioimaging Lab, Dept. of Instrumentation and Applied Physics, Indian Institute of Science, Bangalore

²Dept. of Physics, Indian Institute of Science, Bangalore

³Dept. of Molecular Reproduction and Development Group, Indian Institute of Science, Bangalore

KEY WORDS : Light sheet microscopy, Image Reconstruction, 3D Imaging.

Frequent and long time monitoring is essential for studying rapidly occurring biological processes. Photobleaching is one of the major concerns in these situations. In order to address this issue, we demonstrate a limited-view light sheet microscopy (LV-LSM) for three dimensional (3D) volume imaging. Unlike the existing techniques for 3D imaging, we have taken limited angular views (18 views) of the macroscopic specimen. Instead of taking translational views as done in existing techniques, we rotate the specimen over 180^0 [1]. Post processing with maximum likelihood (ML) technique is employed for reconstructing a high quality 3D volume image. Existing variants of light-sheet microscopy require approximately 10-fold more images to render a 3D volume image. Moreover, LV-LSM technique reduces data acquisition time and consequently minimizes light-exposure by many-folds and thus improves temporal resolution. Results show noise-free and high contrast volume images when compared to Selective Plane Illumination Microscopy (SPIM).

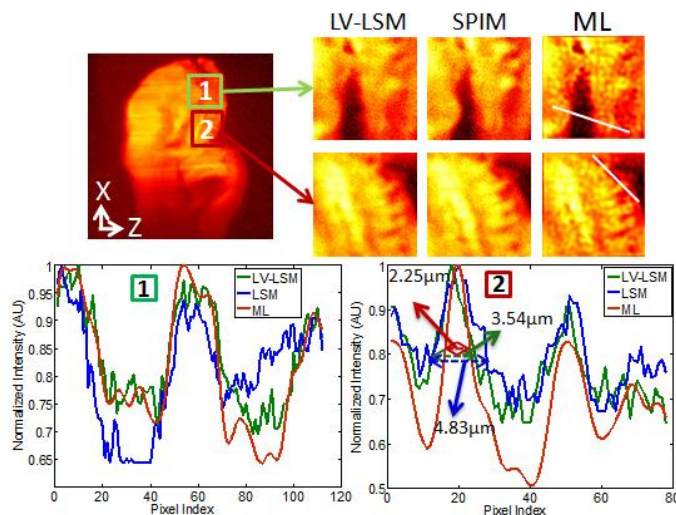


Figure 1 shows two cropped regions (1 & 2) from the angular views. Five day old zebrafish embryo is considered for our study. ML reconstructed images are also shown along with the LV-LSM and SPIM images. Intensity line plots are shown along the white lines drawn on the images. Noise reduction and improved contrast are evident from the line plots. Feature preservation is also evident from the line plots. 3D image is constructed from 18 angular views with 10^0 angular separation.

- [1] J. Huisken, J. Swoger, F. DelBene, J. Wittbrodt, E. H. K. Stelzer, "Optical sectioning deep inside live embryos by selective plane illumination microscopy". *Science* **305**, 1007-1009 (2004).
[2] C. K. Rasmi, Kavya Mohan, M. Madhangi, K. Rajan, U. Nongthombam, and Partha P. Mondal "Limited-view light sheet fluorescence microscopy for three dimensional volume imaging", *Applied Physics Letters* **107**, 263701 (2015).

Evidence of Nanoscale dynamical domains in model binary lipid bilayers

Roobala and Jaydeep K Basu

Department of Physics, IISc, Bangalore, India

E-mail: basu@physics.iisc.ernet.in

Dynamic heterogeneity in model lipid membranes gives insight about the universal nature of correlated systems like glass formers ^[1] or cell membrane ^[2] etc. Several studies have looked at the similarities between the lipid membranes and glass forming fluids ^[3]. We have tried to address the question of dynamic heterogeneity in a simple two component (DLPC: DPPC) supported lipid bilayer using a combination of studies like STED, FCS and AFM. We vary the composition of DLPC and DPPC lipid bilayers and discuss how dynamical lipid domains on the scale of 80-150 nm emerge in these bilayers depending on their composition as well as on the phase in which the domains exist.

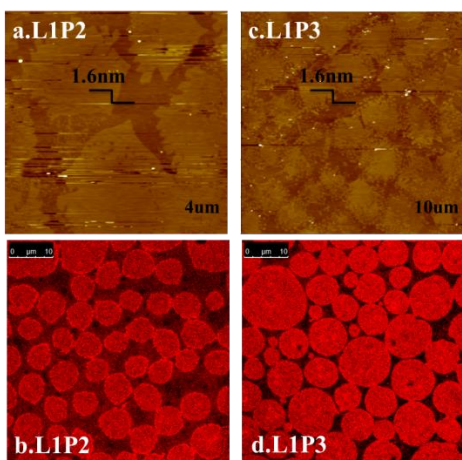


Fig 1: Phase structures obtained from AFM and confocal vs focal area

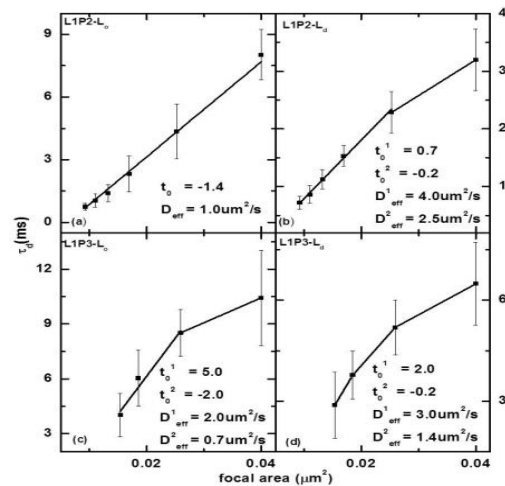


Fig 2 : STED FCS results: transit time

Fig 1 shows the phase structures obtained using AFM (a, c) and confocal (b, d) in case of high DPPC fraction. Fig 2 shows results from STED-FCS experiments on corresponding samples. Transit time should follow a linear dependence on focal area with a zero intercept for normal diffusion. Any deviation from this is interpreted ^[4] to be due to the presence of small scale domains in the observation area. STED-FCS could detect presence of nanoscale domains even in cases not captured under AFM. In high DPPC fraction, strong signatures for presence of nanodomains are observed. These nanodomains are neither an effect of line tension nor validate the property of a thermodynamic phase; rather they are like dynamic clusters that occur in glass forming liquids ^[5]. Such islands of lipids with transient properties different from its environment also plays a significant role in cellular membrane related processes.

References:

- [1] Ediger, M. D. *Annu. Rev. Phys. Chem.* 2000, **51**, 99–128
- [2] Simons, K.; Ikonen, E. *Nature* 1997, **387**, 569–572
- [3] Starr, F. W.; Hartmann, B.; Douglas, J. F. *Soft Matter* 2014, **10**, 3036–3047
- [4] Favard, C.; Wenger, J.; Lenne, P.-F.; Rigneault, H. *Biophysical journal* 2011, **100**, 1242–1251
- [5] Shafique, N., Kennedy, K. E., Douglas, J. F., & Starr, F. W.; *The Journal of Physical Chemistry B* (2016)

Berezinski-Kosterlitz-Thouless transition in thin superconducting films

Pratap Raychaudhuri

Tata Institute of Fundamental Research

(www.tifr.res.in/~superconductivity)

This year's Nobel Prize was shared by David Thouless and Michael Kosterlitz and Duncan Haldane for their seminal work on topological phase transition and topological phases of matter. One of the pioneering work listed in the Nobel citation is the Kosterlitz-Thouless transition, or more precisely the Berezinski-Kosterlitz-Thouless (BKT) transition (independently also predicted by Vadim Berezinski): A new class of phase transitions predicted in 2-dimensional systems that does not break any continuous symmetry. Physical realization of BKT transition has since been obtained in superfluids, superconductors, Bose-Einstein condensates of cold atoms and 2-D single crystals.

In this talk, I will start with a historical overview of the seminal work of BKT and then describe our own experiments on the realization and detection of BKT transition in thin superconducting films. Along the way I will also take you through a simple yet powerful toy, the two-coil mutual inductance setup that allowed us to measure the superfluid density and its temperature dependence in thin superconducting films.

Ref:

Appl. Phys. Lett. **96**, 072509 (2010); Phys. Rev. Lett. **107**, 217003 (2011); Phys. Rev. Lett. **111**, 197001 (2013); Phys. Rev. B **91**, 054514 (2015)

POSTER ABSTRACTS

Exploding and Imaging Bubbles in Superfluid Helium

Yadav Neha(1), Vadakumbatt Vaisakh(1), Maris Humphrey J.(2), Ghosh Ambarish(3)

1) Indian Institute of Science, Department of Physics, Bangalore, India 560012

2) Brown University, Department of Physics, Providence, Rhode Island 02912

3) Indian Institute of Science, Center For Nano Science And Engineering, Bangalore, India 560012

An electron bubble in liquid Helium-4 under saturated vapour pressure becomes hydrodynamically unstable at a pressure more negative than -1.9 bars, which can be easily achieved with focused sound waves. Here, we report on imaging the cavitation of an electron bubble at 30000 frames per second, which reveals that the bubbles can grow to as large as 1 mm within 2 ms of the cavitation event. As revealed from our numerical simulations, the inertia of the bubble wall during cavitation plays an important role in determining its maximum size. The dependence on temperature and static pressure within the experimental chamber will also be discussed.

Corresponding author email: nehayadav0020@gmail.com

Factors influencing the PVC-triggering ability of a cluster of early afterdepolarization-capable myocytes: A computational study

Soling Zimik, Alok Ranjan Nayak, Rahul Pandit

Abstract

Premature ventricular complexes (PVCs), which are abnormal impulse propagations in cardiac tissue, can develop because of various reasons including early afterdepolarizations (EADs). We show how a cluster of EAD-generating cells (EAD clump) can lead to PVCs in a model of cardiac tissue, and also investigate the factors that assist such clumps in triggering PVCs. In particular, we study, through computer simulations, the effects of the following factors on the PVC-triggering ability of an EAD clump: (1) the repolarization reserve (RR) of the EAD cells; (2) the size of the EAD clump; (3) the coupling strength between the EAD cells in the clump; and (4) the presence of fibroblasts in the EAD clump. We find that, although a low value of RR is necessary to generate EADs and hence PVCs, a very low value of RR leads to low-amplitude EAD oscillations that decay with time and do not lead to PVCs. We demonstrate that a certain threshold size of the EAD clump, or a reduction in the coupling strength between the EAD cells, in the clump, is required to trigger PVCs. We illustrate how randomly distributed inexcitable obstacles, which we use to model collagen deposits, affect PVC-triggering by an EAD clump. We show that the gap-junctional coupling of fibroblasts with myocytes can either assist or impede the PVC-triggering ability of an EAD clump, depending on the resting membrane potential of the fibroblasts and the coupling strength between the myocyte and fibroblasts.

Coherent population trapping (CPT) versus electromagnetically induced transparency (EIT)

Sumanta Khan*, MP Kumar, Vineet Bharti, and Vasant Natarajan

Department of Physics, Indian Institute of Science, Bangalore - 560012,

Abstract

We discuss the differences between two well-studied and related phenomena—coherent population trapping (CPT) and electromagnetically induced transparency (EIT). Many differences between the two—such as the effect of power in the beams, detuning of the beams from resonance, and the use of vapor cells filled with buffer gas—are demonstrated experimentally. The experiments are done using magnetic sublevels of the $1 \rightarrow 1$ transition in the D₂ line of ⁸⁷Rb.

Keywords: Electromagnetically induced transparency; Coherent population trapping; Coherent control; Quantum optics.

*E-mail: sumantakhan@physics.iisc.ernet.in

Field emission properties and strong localization effect in conduction mechanism of nanostructured perovskite LaNiO₃

Ramesh B.Kamble, Narendra Tanty, Ananya Patra and V.Prasad

We report the potential field emission of highly conducting metallic perovskite lanthanum nickelate (LaNiO₃) from the nanostructured pyramidal and whisker shaped tips as electron emitters. Nano particles of lanthanum nickelate (LNO) were prepared by sol-gel route. Structural and morphological studies have been carried out. Field emission of LNO exhibited high emission current density $J=3.37 \text{ mA/cm}^2$ at a low threshold electric field $E_{th}=16.91 \text{ V}/\mu\text{m}$, obeying Fowler-Nordheim tunneling. The DC electrical resistivity exhibited upturn at 11.6 K indicating localization of electron at low temperature. Magnetoresistance measurement at different temperatures confirmed strong localization in nanostructured LNO obeying Anderson localization effect at low temperature.

Phase transitions in organic crystal Di-isopropyl-ammonium Iodide

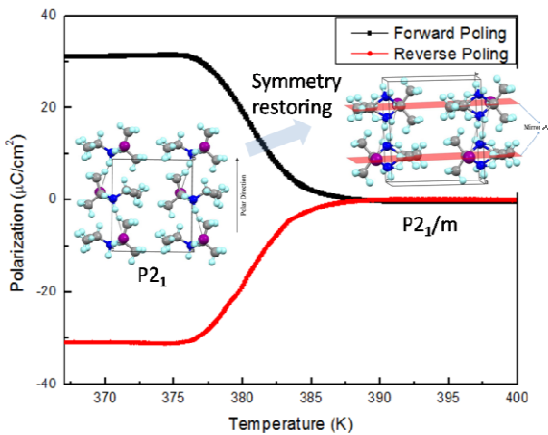
Ravi Saripalli^{1*}, Dipti Swain², Siva Prasad¹, Hari Haran N.¹, T.N.Guru Row², H.L.Bhat¹, Suja Elizabeth¹

¹Department of Physics, Indian institute of science, Bangalore, India

²Solid State and Structural Chemistry Unit, Indian Institute of Science, Bangalore, India

*Department of Physics, Indian institute of science, Bangalore – 560012, India,
rksaripalli@physics.iisc.ernet.in

ABSTRACT



Recent investigations on simple organic, molecule based ferroelectric material namely, di-isopropyl-ammonium chloride (abbreviated as DPC) [Adv. Mater. 2011, 23, 5658–5662] and di-isopropyl-ammonium bromide (abbreviated as DPB) [Science 2013, 339, 425], reveal high Curie temperatures (T_c) of 440 K and 425 K respectively. Their ferroelectric activity commences below T_c with large spontaneous polarization (P_s) of $8.9 \mu\text{Ccm}^{-2}$ and $23 \mu\text{Ccm}^{-2}$ respectively. The spontaneous polarization of DPB is comparable to that of Barium Titanate ($P_s = 26 \mu\text{Ccm}^{-2}$) [Nat. Mater. 2008, 7, 357–366]. Organic molecular ferroelectric materials are popular due to light weight, easy fabrication and growth, environmental-friendly processing and mechanical flexibility, which make them potential candidates for applications in organic electronics. The fact that DPB exhibits strong ferroelectricity suggests that other simple organic analogs may have comparable ferroelectric properties to those encountered in inorganic ferroelectrics. In this work, a closely related iodine analog to DPB and DPC, Diisopropylammonium iodide has been synthesized and studied for ferroelectric properties.

Diisopropylammonium Iodide (DPI) crystals were first grown by mixing Diisopropylammonium and 57% hydroiodic acid in equimolar ratio. Polycrystalline samples of DPI were obtained after slow evaporation of the mixture in 6 days, which were recrystallized in ethanol solution to obtain single crystals. DPI showed two reversible phase transitions which have been identified by DSC and dielectric measurements. Single crystal x-ray diffraction studies were carried out using an Oxford Xcalibur diffractometer with Eos detector and Mova microsource (Mo-K α radiation, Lambda = 0.71073 Å). The diffractometer is equipped with Oxford Cobra open stream non-liquid nitrogen device for high temperature data collection. The structure was solved by direct methods in Shelx-2014. From the detailed structural studies it was found that the first transition at 367 K is from orthorhombic $P2_12_12_1$ to monoclinic $P2_1$. The polar $P2_1$ phase is ferroelectric as evidenced by the pyroelectric measurements and showed very high magnitude of spontaneous polarization ($P_s = 30 \mu\text{Ccm}^{-2}$), which is higher in comparison to the bromide and chloride analogs, other organic molecular ferroelectrics and even inorganic BTO. The second transition at 410 K is from polar monoclinic $P2_1$ space group to non-polar monoclinic $P2_1/m$. Thus DPI is an organic ferroelectric with very high spontaneous polarization and a high Curie temperature.

Raman study of pressure induced phase transitions in SnTe

Sukanya Pal¹, Sandhya Shenoy², Subhajit Roychowdhury³,
Kaniska Biswas³, D.V.S. Muthu¹, U.V. Waghmare², and A.K.Sood¹

November 8, 2016

¹*Department of Physics, Indian Institute of Science, Bangalore 560012, India*

²*Theoretical Science Unit, Jawaharlal Nehru Center for Advanced Scientific Research, Jakkur P.O., Bangalore 560064, India*

³*New Chemistry Unit, Jawaharlal Nehru Center for Advanced Scientific Research, Jakkur P.O., Bangalore 560064, India*

(Abstract for Poster)

Abstract

Topological crystalline insulators (TCI) are new class of materials which have attracted interest because of their interesting topology. They are characterized by bulk band gap with metallic surface states which are protected by mirror symmetry. TCIs are different from topological insulators(TI)where the surface states are protected by the time reversal symmetry. Tin telluride (SnTe), a narrow band-gap (0.18 ev) semiconductor has recently been discovered to be TCI and thus it attracted our attention towards it. At ambient conditions SnTe crystallizes in cubic Fm-3m structure and with temperature and pressure variations it can undergo structural and electronic transitions.

We report Raman study of SnTe as a function of pressure up to 25GPa at room temperature. The strongest mode near 126 cm^{-1} shows anomalous softening upto 1.8 GPa, accompanied by an increase in the line width, confirming a pressure induced electronic topological transition (ETT) reported earlier by resistivity, x-ray diffraction studies and the first-principles calculations showing a band-gap closure. It also no longer remains a TCI, indicating a topological phase transition. At the onset of ETT two new Raman modes near 55 cm^{-1} and 126 cm^{-1} also appear, indicating a first order structural phase transition. Further structural transitions are observed at ~ 5 GPa, ~ 12 GPa and ~ 18 GPa as marked by the change in slope of Raman frequencies with pressure and sharp discontinuities in the frequencies.

Understanding Dendrimer-Graphene Composite for Supercapacitor Application

Mounika Gosika¹, Taraknath Mandal², and Prabal K. Maiti¹

¹Center for Condensed Matter Theory, Department of Physics,
Indian Institute of Science, Bangalore - 560012

²Department of Chemical Engineering, University of Michigan,
Ann Arbor - 48109

Abstract

Increasing the energy density in capacitive energy storage devices has been of great practical interest in the recent years. The well-defined molecular structure and flexibility in the size, shape make dendrimers the potential candidates as electrolytes in these devices [1]. Therefore, it is crucial to understand the dynamics of dendrimers on an electrode's surface.

We have performed fully atomistic molecular dynamics simulations to study the structure and interactions of PAMAM dendrimers on a graphene sheet, in an aqueous environment for generations 3, 4 at low, neutral and high pH levels. We observe that the dendrimers undergo significant structural changes upon adsorption, acquiring a pancake type flat structure, as opposed to their well-known spherical geometries in bulk. We report the first finding of Sombrero-type structures, predicted theoretically [2] and also observed computationally [3] in the context of star-polymer adsorption, for neutral pH dendrimers. We have also studied the effective interactions between the adsorbed dendrimers. The free energies quantified using umbrella sampling calculations suggest that the interactions between the dendrimers are always repulsive irrespective of the protonation level, contrary to the attractive interaction observed for high pH dendrimers in bulk [4]. We show that stronger dendrimer-graphene interaction compared to dendrimer-dendrimer interaction is responsible for such behaviour.

References

- [1] Lin, Terri C. (2013). Poly(amido amine) Dendrimers in Supercapacitors. doi:10.2172/1091321
- [2] A. Halerpin, J. F. Joanny, J. Phys. II France. **1**(6), 623 (1991).
- [3] A. Chermos et al., Soft Matter. **6**, 1483 (2010).
- [4] T. Mandal et. al., J. Chem. Phys. **141**, 144901 (2014).

A theoretical study of the build-up of the Sun's polar magnetic field by using a 3D kinematic dynamo model

Gopal Hazra, Arnab Rai Choudhuri and Mark Miesch

November 9, 2016

Abstract

We develop a three-dimensional kinematic self-sustaining model of the solar dynamo in which the poloidal field generation is from tilted bipolar sunspot pairs placed on the solar surface above regions of strong toroidal field by using the SpotMaker algorithm and then the transport of this poloidal field to the tachocline is primarily caused by turbulent diffusion. We obtain a dipolar solution within a certain range of parameters. We use this model to study the build-up of the polar magnetic field and show that some insights obtained from surface flux transport (SFT) models have to be revised. We present results obtained by putting a single bipolar sunspot pair in a hemisphere and two symmetrical sunspot pairs in two hemispheres. We find that the polar fields produced by them disappear due to subduction by the meridional circulation sinking underneath the surface in the polar region, which is not included in the SFT models. We also study the effect that a large sunspot pair violating Hale's polarity law would have on the polar field. We find that there would be some effect—especially if the anti-Hale pair appears at high latitudes in the mid-phase of the cycle—though the effect is not very dramatic.

The Tenfold Way: A Group Cohomological View

Vijay B. Shenoy,* Adhip Agarwala, and Arijit Haldar

Physics Department, IISc Bangalore

(Dated: November 10, 2016)

Abstract

Fermionic systems can possess “intrinsic” symmetries like time reversal, charge conjugation and sublattice. We show how such symmetries arise from the structure of the Hilbert-Fock space and conclude that such symmetries are described by the Klein group \mathcal{K}_4 ($= Z_2 \times Z_2$) or its subgroups. We show that the ten symmetry classes arise as projective representations of \mathcal{K}_4 and its subgroups by a group cohomological analysis. We briefly discuss how these insights can help understand topological phases of interacting fermions.

Reference: arXiv:1606.05483

* shenoy@physics.iisc.ernet.in

Direct evidence of tunable 1d superlattice in graphene probed by Magneto-capacitance measurements

Manabendra Kuiry¹, Chandan Kumar¹ and Anindya Das¹

¹*Department of Physics, Indian Institute of Science, Bangalore 560012, India*

Abstract

Superlattice potential modifies the band structure of graphene, leading to tailored electronic properties. Graphene placed on hexagonal boron nitride with accurate alignment along its crystallographic axis show Moiré pattern which act as superlattice potential, leading to the modulation of band structure in graphene. However, they lack the tunability of superlattice potential. Here we have realized tunable graphene superlattice using periodic array of gates with a period of ~ 100 nm. In this work, we have employed resistance measurement together with quantum capacitance measurement in the presence of magnetic field to investigate the evolution of Landau levels as function of superlattice potential. At zero superlattice potential we see the conventional Landau fan diagram of graphene, but with the application of superlattice potential, there is a mixing of landau levels depending on the strength of the superlattice potential. Quantum capacitance is directly proportional to the density of states, which indicates the modulation of band structure with superlattice potential.

*email: manab@physics.iisc.ernet.in

Probing in-plane anisotropy in 2D ReS₂ flakes using conductance and low frequency noise measurement

Richa Mitra and Anindya Das

Department of Physics, Indian Institute of Science, Bangalore 560012, India

Abstract

Transition metal Dichalcogenides are emerging as promising material for various electronic and optoelectronic applications because of its unique structural and electrical properties. TMDCs have chemical formula MX₂ (M=Metal atom, X=chalcogen atom) where two layers of chalcogen atoms sandwich one metal atom layer in between. ReS₂ is the new member of the TMDC family. It is an n-type semiconducting material with 1.4 eV direct bandgap. ReS₂ crystalizes into a unique 1T' phase which is distorted 1T structure. Peierls transition of 1T structure leads to the formation of 1T' phase with zigzag one-dimensional Re chains in the basal plane of the crystal. This less symmetric structure of ReS₂ leads to highly anisotropic electronic, optical property unlike conventional TMDCs. We have probed the in-plane anisotropy of ReS₂ by 2 probe conductance measurement and low frequency 1/f noise measurement. Anisotropy in conductance and noise are quantified and compared. The noise measurement shows higher sensitivity towards anisotropy than conductance measurement. The noise anisotropy has been analysed in terms of mobility dependence on noise figure. Also schottky barrier height at the contact has been extracted from temperature varying conductance measurement and its possible influence on two probe conductance and noise has been discussed.

Probing Photo-Induced Conductivity in Bismuth Telluride Nanowires Using Time Resolved Optical Pump Terahertz Probe Spectroscopy

Mithun K P¹, Srabani Kar¹, Abhinash Kumar², Subhajit Kundu², N Ravishankar² and A K Sood¹

¹Centre for Ultrafast Laser Applications, Indian Institute of Science, Bangalore 560012

²Material Research Centre, Indian Institute of Science, Bangalore 560012

ABSTRACT

We study the relaxation dynamics of photo-excited carriers in Bismuth Telluride Nanowires (Bi_2Te_3 NWs) using Time resolved Optical Pump Terahertz Probe (OPTP) spectroscopy. The measured differential photo-induced complex conductivity is best described using the Lorentian model, showing fluence and delay dependent resonance frequency shift from 1-3.5THz as depicted in fig[1]. Such a shift in the resonance frequency with respect to fluence and delay time is very similar to the behaviour of Surface Plasmons Oscillations (SPO)¹. Hence, we attribute these Lorentzian peaks to the Localized Surface Plasmon modes (LSP). After photo-excitation with 800 nm pump, a decrease in the terahertz transmission is observed due to absorption of the THz radiation by photo-excited charge carriers. The non-equilibrium carriers shows a pump fluence independent relaxation with two distinct time scales; a faster relaxation (~8ps) attributed to the direct recombination of electron-hole pairs and a larger relaxation time scale (~34ps) contributed by surface trap states inbuilt in the nanowires due to their large surface area to volume ratio (fig[2]).

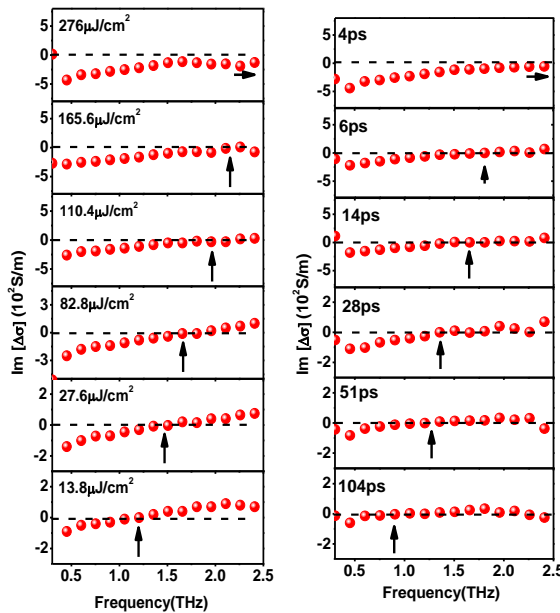


Figure 1 : The imaginary part of the differential photo-induced complex conductivity is plotted (a) at different pump fluences and (b) at different pump-probe delay time. The black arrow shows the shift in the resonance frequency.

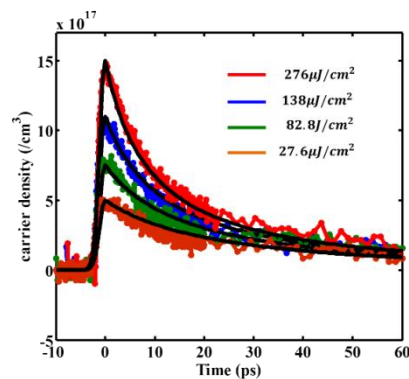


Figure 2: the optical pump THz probe signal at different pump fluences. The solid lines are the fits to the relaxation dynamics of the photo-excited carriers

References:

- P.Parkinson, J.L.Hughes, Q.Gao, H.H.Tan, C.Jagadish, M.B.Johnston and L.M.Herz, *Transient Terahertz Conductivity of GaAs Nanowires*, Nano Lett. 7,7,2162-2165 (2007)

Dendrimers as nanoscale blockers for the toxic cytolysin A (ClyA) protein pores

Subbarao Kanchi^{a,b}, Taraknath Mandal^a, K. G. Ayappa^b, and Prabal K. Maiti^a

^aCenter for Condensed Matter Theory, Department of Physics, Indian Institute of Science, Bangalore 560012, India.

^bDepartment of Chemical Engineering, Center for Biosystems Science and Engineering, Indian Institute of Science, Bangalore 560012, India.

Abstract

Designing effective nanoscale blockers for membrane inserted pores formed by pore forming toxins (PFTs), which are expressed by several virulent bacterial strains, on a target cell membrane is a challenging and active area of research. In this study, we demonstrate that PAMAM and PETIM dendrimers can be effectively used as blocking reagents for the toxic cytolysin A (ClyA) protein pores. We have performed all-atom molecular dynamics (MD) simulations to characterize the ClyA protein pores modified with PAMAM and PETIM dendrimers of generations G3,G5 and G4,G6 respectively. Our results show that apart from non-protonated G4 PETIM, all PAMAM and PETIM dendrimers can spontaneously enter the pore lumen in either of their protonated (P) or non-protonated (NP) states. Protonated dendrimers interact strongly with the negatively charged protein pore lumen. As a consequence, P dendrimers assume a more expanded configuration efficiently blocking the pore when compared with the more compact configuration adopted by the neutral NP dendrimers creating a greater void space for the passage of water and ions[1]. The ions/water flux through the pore is generated by applying a weak force and the pore blockage is quantified by computing their conductance as well as the residence times. The high generation dendrimers (G5 PAMAM and G6 PETIM) are more efficiently blocking pore and ionic currents are reduced by 91% for the P dendrimers and 31% for the NP dendrimers. The preferential binding of Cl^- counter ions to the P dendrimer creates a zone of high Cl^- concentration in the vicinity of the internalized dendrimer and a high concentration of K^+ ions in the transmembrane region of the pore lumen. In addition to steric effects, this induced charge segregation for the P dendrimer effectively blocks ionic transport through the pore. The free energy profiles of dendrimers along the pore axis are calculated to find their binding energies. The NP dendrimers enter deeper into the pore and strongly bind to the lumen, while P dendrimers bound near the extracellular pore entrance. The ion conductance and free energy profiles conclude that the PAMAM dendrimers are relatively more efficient in blocking the pore compared with the PETIM dendrimers. The bio-compatible PAMAM/PETIM dendrimers can potentially be used to develop therapeutic protocols based on the pH sensitive gating of pores formed by pore forming toxins to mitigate bacterial infections.

References

- [1] T. Mandal, S. Kanchi, K. G. Ayappa and Prabal K. Maiti, *Nanoscale* **8**, 13045–13058 (2016).

Structure, Micrograph and Transport Properties of Bi_2Te_3 added CoSb_3

Sanyukta Ghosh^a, B. S. Murty^b, Ramesh Chandra Mallik^{a*}

^aThermoelectric Materials and Devices Laboratory, Department of Physics, Indian Institute of Science, Bangalore-560012

^bDepartment of Metallurgical and Materials Engineering, Indian Institute of Technology, Madras, Chennai-600036

*Email: rcmallik@physics.iisc.ernet.in

Abstract:

Skutterudite based thermoelectric materials have drawn great attention recently due to their ability to convert heat into electricity. Among all the thermoelectric materials, binary skutterudite with chemical formula MA_3 ($\text{M}=\text{Co, Ir, Rh}$ and $\text{A}=\text{P, As, Sb}$) with space group $Im\bar{3}$ have shown interesting thermoelectric properties at mid temperature range (400-750 K). It satisfies most of the properties of good thermoelectric material such as, large unit cell, high atomic masses, high carrier mobility, and covalent bond between constituent atoms. At the same time it has low power factor (due to low electrical conductivity) and high thermal conductivity (due to high lattice part of thermal conductivity) as compared to other thermoelectric materials. Nano inclusion in skutterudite can lead to higher electrical conductivity by increasing carrier concentration and lower phonon thermal conductivity by scattering phonons effectively. $\text{Co}_4\text{Sb}_{12}$ was prepared by induction melting at 1130 K followed by annealing at 973K for 168 hours. Pre-synthesized Bi_2Te_3 powder mixed with $\text{Co}_4\text{Sb}_{12}$ powder according to the chemical formula $(\text{Bi}_2\text{Te}_3)_x\text{Co}_4\text{Sb}_{12}$ (where $x=0.1, 0.2, 0.3, 0.4$) was ball milled for 1 hour. The composite powder was sintered by Spark Plasma Sintering (SPS) at 873 K under vacuum of 0.5 mbar. X-ray diffraction (XRD) pattern confirms the presence of Bi_2Te_3 secondary phase with CoSb_3 main phase. The surface morphology of the samples were investigated by Scanning Electron Microscopy (SEM) and compositions were detected by Electron Probe Micro Analyzer (EPMA) which is in good agreement with XRD results. In addition, Sb secondary phase was observed in EPMA for samples with $x \geq 0.2$. High temperature XRD was carried out between 300 K and 723 K. Rietveld refinement showed that lattice parameters are increasing with temperature and using these data the thermal expansion coefficient was calculated. The Seebeck coefficient (S) and electrical resistivity (ρ) were measured by the differential method and four probe method respectively, using Linseis LSR-3 in the temperature between room temperature and 750 K. S is negative for all the samples indicating n type of semiconductor. Both S and ρ increase with increasing temperature upto about 450 K and thereafter decrease due to bipolar conduction. Moreover, with increasing Bi_2Te_3 content ρ decreases and the maxima of S shifts towards higher temperature due to increased carrier concentration which is confirmed by the Hall measurement data. Maximum power factor (S^2/ρ) of 0.83mW/mK^2 at 452 K has been achieved for sample with $x=0.3$ which is higher than pure CoSb_3 (0.3 mW/mK^2 at 700 K) [1] and lower than pristine Bi_2Te_3 (2.92mW/mK^2 at 300 K) [2].

References:

- [1] Feng B., Xie J., Cao G., Zhu T., & Zhao X. Enhanced thermoelectric properties of p-type CoSb_3 graphene nanocomposite. *Journal of Materials Chemistry A*, **1**(42), 13111-13119, (2013).
- [2] Liu, W., Lukas, K. C., McEnaney, K., Lee, S., Zhang, Q., Opeil, C. P., & Ren, Z. Studies on the $\text{Bi}_2\text{Te}_3-\text{Bi}_2\text{Se}_3-\text{Bi}_2\text{S}_3$ system for mid-temperature thermoelectric energy conversion. *Energy & Environmental Science*, **6**(2), 552-560, (2013).

Novel photo-tunable transfer characteristics in MoTe₂-MoS₂ vertical hetero-structure

Authors:

Arup Kumar Paul, Manabendra Kuiry, Dipankar Saha, Biswanath Chakrobarti, Santanu Mahapatra,
A.K Sood, and Anindya Das,

Abstract for poster:

Conduction through vertical van der Waals p-n junction is different from that of conventional p-n junction. Here transport is determined by recombination process via inter-layer tunneling of carriers. Hence the control and tunability of the inter-layer tunneling rate in these p-n junctions has a potential to exhibit new kind of electronic and opto-electronic devices. Here, we present electrical and opto-electrical measurements on few-layers MoTe₂(p) - single layer MoS₂(n) hetero-junction. The trans-conductance of the hetero-junction as a function of gate voltage reveals an unusual dip at the highest conductance value. The magnitude of the dip in trans-conductance depends on the incident power density of light. Our devices show very high photoresponsivity of $\sim 10^5$ A/W at room temperature, highest so far in TMD-TMD vertical heterostructures. These observations with a simple model shows how the inter-layer recombination rate dependent on the effective carrier concentration (tuned by light intensity), controls the transport in these junctions. In addition, we have also conducted an atomistic study in order to explore the charge carrier transport through MoS₂-MoTe₂ van der Waals (vdW) hetero-structures. The results obtained, using density functional theory (DFT) - non equilibrium Green's function (NEGF) method, to capture the dip in the transmission spectra.

Understanding DNA Based Nanostructures using Molecular Simulations

Himanshu Joshi and Prabal K. Maiti

Centre for Condensed Matter Theory, Department of Physics, Indian Institute of Science,

Bangalore 560 012, India

DNA is arguably the most important biological molecule. Recent decades have witnessed the synthesis of many DNA nanostructures with proposed applications in nanotechnology. State of the art molecular dynamics (MD) simulations can be very useful to understand the microscopic structure of these self-assembled structures at nanoscale. We have developed algorithms to build very accurate 3-d atomistic models of various DNA nanostructures like crossover DNA molecules, DNA nanotubes (DNTs) and DNA polyhedra. We investigate the structure, stability and mechanical properties of various DNA nanostructures in salt solution. We find that the persistence length of DNA nanotubes is of the order of micrometer. We have also examined the interaction of DNA nanotubes embedded in the lipid bilayer membranes. We discover that the local rearrangement of lipid molecules can stabilize the DNA nanotubes in the bilayer and DNA backbone modification is not necessary for the partitioning of DNTs in lipid bilayer. The Ohmic conductance measured from I-V characteristics of the ions channel varies from 4.3 to 20.6 nS with ionic strength. The simulation studies with atomistic model of DNA icosahedron reveal the dynamical behavior of the structure and its interaction with encapsulated cargo. We believe that our MD simulation studies will give further impetus in the development of structural DNA nanotechnology.

Semiconducting Conjugated Microporous Polymer, Poly(1,3,5 triethynylbenzene):

Photoelectrochemical Water Splitting, Oxygen Reduction and Supercapacitors

Swetha Jayanthi^a, D. Victor S. Muthu^b, N. Jayaraman^c, S. Sampath^d and A. K. Sood^b

^aCentre for Nano Science and Engineering, ^bDepartment of Physics, ^cDepartment of Organic Chemistry, ^dDepartment of Inorganic and Physical Chemistry

Intriguing structural design and inherent nanoporosity of conjugated microporous polymers (CMP) with extended π -conjugation have stimulated research interest in exploring their applications to solve challenging environmental and energy problems. However, only few attempts are made so far to identify the semiconducting properties of these CMP networks having direct relevance to energy conversion, electronic devices and photocatalysis. The present study identifies the semiconducting properties of a CMP, namely, poly(1,3,5-triethynylbenzene) (PTEB) in detail using photoluminescence, UV-Vis absorption, Kelvin probe force microscopy, cyclic voltammetry, Mott-Schottky analysis and photoelectrochemical studies. Fine tuning of the band gap of this network by applying uniform hydrostatic pressures in diamond anvil cell is also demonstrated. Integration of hetero-atoms such as nitrogen into the polymer network by post-thermal treatment is shown to enhance significantly the activities towards oxygen reduction reaction and charge storage capacities in electrochemical capacitors. A drastic improvement in the activity of PTEB observed on nitrogen incorporation into the carbon skeleton is attributed to the increase in number of electrochemical active sites and increase in the pore size of PTEB. The systematic evaluation of conducting properties of CMP materials pave the way for future development of electronic, electrochemical and photoelectrochemical devices.

Statistical Properties of Inertial-Particle Trajectories in 3D Homogeneous and Isotropic Super-fluid Turbulence

Akhilesh Kumar Verma,¹ Akshay Bhatnagar,² Vishwanath Shukla,³ and Rahul Pandit⁴

¹*Center for Condensed Matter Theory, Department of Physics,
Indian Institute of Science Bangalore 560012 India.*

²*NORDITA, Roslagstullsbacken 23, SE-10691 Stockholm, Sweden.*

³*Laboratoire de Physique, ENS de Lyon, Lyon, France.*

⁴*Centre for Condensed Matter Theory, Department of Physics,
Indian Institute of Science, Bangalore 560012, India.*

We study the statistical properties of inertial particles that are advected by the turbulent flow of a super-fluid by carrying out extensive direct numerical simulations (DNSs) of the two-fluid, Hall-Vinen-Bekharevich-Khalatnikov (HVBK) equations. For our DNSs we have developed a pseudo-spectral code to solve the three-dimensional (3D) HVBK equations; this part of our study builds upon earlier DNSs of the 3D Navier-Stokes (NS) for a single-component, viscous fluid. Clearly, a pseudo-spectral DNS of the 3D HVBK is much more difficult than its 3D NS counterpart because, in the former, we must solve a 3D Euler-type equation for the super-fluid velocity u_s along with the 3D NS-type equation for the normal-fluid velocity u_n ; these two equations are coupled by the mutual-friction term.

We use our DNSs to obtain the probability distribution functions (PDFs) of the curvature (κ) and magnitude of the torsion (θ) of heavy-particle trajectories in turbulent, 3D HVBK flows that are statistically steady and homogeneous and isotropic. We show that these PDFs, $P(\kappa)$ and $P(\theta)$, respectively, have power-law tails of the form $P(\kappa) \sim \kappa^{-\alpha_\kappa}$ and $P(\theta) \sim \theta^{-\alpha_\theta}$, for large κ and θ , respectively, where the power-law exponents $\alpha_\kappa \simeq 2.50$ and $\alpha_\theta \simeq 3.0$ seem to be universal numbers, in so far as they are independent of Stokes number of the particles (within our error bars). Furthermore, we show that the PDFs of the angle between the normal-fluid and particle velocities, ϕ_n , and the angle between the super-fluid velocity and the particle velocity, ϕ_s , exhibit power-law regimes in which $P(\phi_n) \sim \phi_n^{-\gamma_n}$ and $P(\phi_s) \sim \phi_s^{-\gamma_s}$, with exponents $\gamma_n \simeq 3.0$ and $\gamma_s \simeq 2.80$. We are studying the dependence (if any) of the these exponents on the mutual friction.

Observation of Andreev reflection at the junction of graphene quantum Hall state and superconductor

Manas Ranjan Sahu, Pratap Raychaudhury, Anindya Das

Abstract for poster

The interface of Quantum Hall (QH) edge state and a superconductor (SC) is a novel route to create topological states like non-abelian Majorana Fermions. The observation of Andreev reflection (A.R) at QH edge state – SC is inevitable to create and manipulate these exotic states. Here we present thorough experimental studies of a system composed of a single layer graphene (SLG) in proximity to two dimensional (2D) superconductor (NbSe_2). The signature of A.R is evident in magnetic fields as high as 10 T at quantum Hall plateau. At such a high magnetic field graphene exhibits degeneracy lifted QH edge states and the conductance becomes zero around $N = 0$ Landau level due to Zeeman induced spin polarized QH edge state, whose role was further verified in tilted magnetic field experiment. However, exactly at the Dirac point an anomalous conductance peak appears in the gate voltage scan and its amplitude increases with temperature in consistent with a compelling evidence of inter-band Andreev reflection. At the end we show the evidence of Andreev edge states. These findings will help to advance the fields in QH-SC, which has application like quantum computing.

Temperature Dependent Charge Transport Study in Hybrid Composite Devices of Organic Semiconductor and Quantum Dots

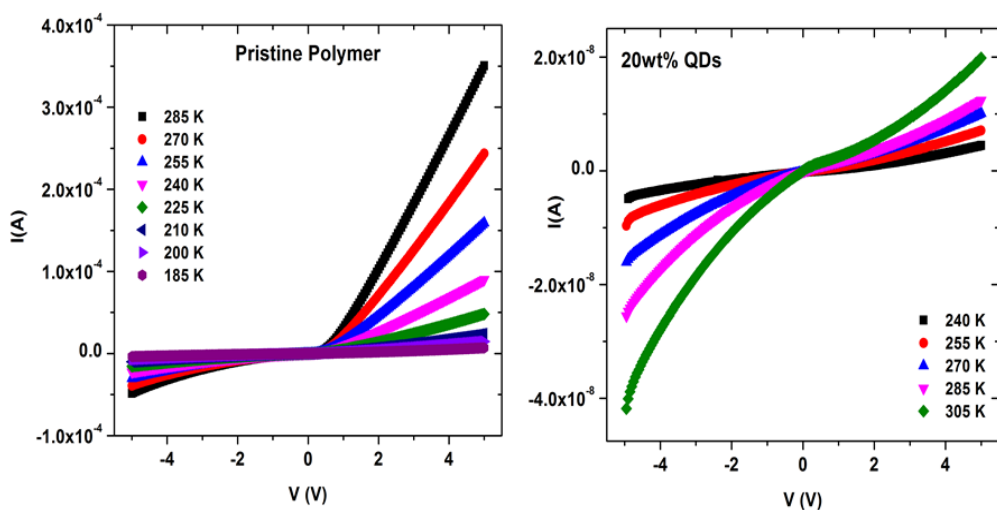
Motiur Rahman Khan*, Amardeep M. Jagtap, K. S. R. Koteswara Rao and R. Menon

Department of Physics, Indian Institute of Science, Bangalore-560012, India

*E-mail: mrkhan.iisc@gmail.com

Organic semiconducting polymer–inorganic nanocrystal composites offer an attractive means to combine the merits of organic and inorganic materials into novel electronic and photonic systems. A study of charge transport and charge transfer phenomena in such hybrid materials is of great importance. Despite the fact that these hybrid materials have garnered tremendous attention for optoelectronic applications, the physics of charge transport in these devices is still not clearly understood. In the present work, nanocomposites are prepared by dispersing silver sulfide (Ag_2S) quantum dots (QDs) in poly (3-hexylthiophene) (P3HT) organic polymer matrix.

Temperature dependent (180 – 300 K) current-voltage measurements are performed on all composite devices in ITO/P3HT- Ag_2S /Au structure. In the pristine device of P3HT, direct tunnelling mechanism is observed at low voltage, whereas thermionic emission is observed at higher voltage in the measured temperature range. Furthermore, highly asymmetric current-voltage characteristics are found at all measured temperatures. In the device of 5 weight percent QDs, the effective barrier is found to increase and further increment is observed in the case of 10 weight percent device as compared to that of pristine. The ratio of forward to reverse bias current is found to decrease with increasing QDs weight percent in P3HT polymer matrix. Interestingly, a transition (decrease in the effective barrier) is observed in the case of 20 weight percent device and the ratio of forward to reverse bias current is found to be less than unity. We have also carried out photoconductivity measurements on the devices made by changing the QDs weight ratio in polymer matrix. A huge increment in the ratio of photocurrent to dark current is observed in the case of 20 weight percent QDs as compared to that of pristine device. Such increment in the photocurrent of hybrid composite devices indicates the effective photo-induced charge separation and transfer between P3HT and Ag_2S QDs.



Raman Spectroscopic Studies on Bismuth Doped Eu₂Ir₂O₇

Anoop Thomas¹, Prachi Telang², Kshiti Mishra², Surjeet Singh², DVS Muthu¹, AK Sood¹

1. Department of Physics, Indian Institute of Science, Bangalore, 560012

2. Indian Institute of Science Education and Research, Pune, 411008

Weyl state is one of the topological phases of matter and is predicted and observed in spin orbit coupled Mott insulator Eu₂Ir₂O₇. The spin orbit driven Mott metal insulator transition takes place at ~120K with all-in-all-out Iridium spin configuration. The metallic state however deviates from normal Fermi liquid behaviour. Application of physical pressure increases bandwidth and generates coherent type electronic excitations. Another way of getting these coherent states is by doping with Bismuth. When Eu³⁺ is replaced by Bi³⁺, an increase in lattice parameter is expected. However an anomalous volume collapse is observed for 2% bismuth doping. The 2% Bi doped Eu₂Ir₂O₇ also shows all-in-all-out type frustrated magnetic ordering in pyrochlore lattice below Mott temperature. Our aim is to study this anomalous behaviour of bismuth doped Eu₂Ir₂O₇ by high pressure and low temperature Raman spectroscopic experiments. At ambient conditions we have seen six Raman active modes in Eu₂Ir₂O₇. A few modes harden for 2% and 10% bismuth doping while two modes soften. We have done high pressure Raman spectroscopic studies on 2% Bi doped sample upto ~28GPa. We are in the process of analysing the data.

Electrical switching, local structure and thermal crystallization in Al-Te glasses

Pumlianmunga, R. Ramanna and K. Ramesh

¹Department of Physics, Indian Institute of Science, Bangalore 560012, India.

Bulk $\text{Al}_x\text{Te}_{100-x}$ glasses ($17 \leq x \leq 29$) prepared by melt quenching method are found to exhibit threshold switching. The local coordination of Al probed by MAS NMR indicates that Al resides in $^{[4]}\text{Al}$, $^{[5]}\text{Al}$ and $^{[6]}\text{Al}$ environments. With the addition of Al, there is an increase in C_3^+ defect centers which largely influences the switching properties of Al-Te glasses. The presence of higher coordinated Al cross-links the network and the network becomes rigid. The switching voltage, glass transition and crystallization temperatures are found to increase with the increase of Al concentration. This indicates that the cross-linking and the rigidity of the structural network increase by the addition of Al. A memory switching material undergoes structural change between amorphous and crystalline states meaning a large structural reorganization. In a highly cross-linked rigid network, structural reorganization becomes difficult and hence results in threshold switching

Shear induced 3D ordering and instabilities in Surfactant Mesh Phases: Coupling between flow and membrane defects.

Mesh phases are formed by a one dimensional (1D) stack of perforated bilayers with liquid-like or hexagonal ordering of perforations in the bilayer plane as in the random or rhombohedral mesh phases. Known since 1960s in different classes of amphiphilic systems comprising surfactants, lipids, diblock copolymers, thermotropic liquid crystals and more recently in star branched polyphiles, their response to shear flow has hardly been addressed. This is despite their structural similarity with bilayer forming phases where shear flow can couple with thermal undulations of the bilayers to give rise to various hydrodynamic instabilities accompanied by structural transitions [1,2].

I will present our recent in-situ Rheological X-ray scattering and small angle light scattering (Rheo-SALS) studies [3] on random mesh and Rhombohedral ($\bar{R}\bar{3}m$) mesh phases where shear can induce in plane as well as out of plane correlation between curvature defects in random mesh phase and form ordered $\bar{R}\bar{3}m$ under shear. On the other hand $\bar{R}\bar{3}m$ phase under shear goes to buckled $\bar{R}\bar{3}m$. We further show that the buckling of the bilayers results in microstructural transitions to multi-lamellar cylinders. A detailed shear diagram (shear stress σ vs volume fraction ϕ) outlining the various shear induced structural transitions in the surfactant mesh phases of a cationic-anionic mixed surfactant system will be presented.

References:

- [1] L. Porcar, W. A. Hamilton, and P. D. Butler, *Langmuir* **19**, 10779 (2003) and references therein.
- [2] V. Rathee, R. Krishnaswamy, A. Pal, M. Imperor, B. Pansu, V. A. Raghunathan, and A. K. Sood, *Proc. Natl. Acad. Sci. USA*, **110**, 14849 (2013).
- [3] Pradip Kumar Bera, Vikram Rathee, Rema Krishnaswamy and A. K. Sood
(manuscript in preparation).

Magnetic field assisted magnetization reversal in permalloy nanoring–nanowire structures

Manohar Lal, S. Sakshath and D. Venkateswarlu

Reliable manipulation of the domain configurations is a central theme of magnetic memory devices. The ring geometry is particularly interesting due to the minimal stray field interference between individual structures in densely packed devices. But the flux-closure domain states, which minimize the stray fields, need to be stabilized by suitable modifications of the ring structures. Here, we explore controllable magnetic field-induced switching between the various domain states in permalloy nano-ring structures, whose flux-closure states are stabilized using nano-wires. Using magneto-resistance measurements, we study the switching field behavior of these structures and perform micromagnetic simulations to validate our experimental findings.

The devices were fabricated by high resolution nano-lithography followed by DC magnetron sputter deposition of NiFe 20 nm/Au 4nm on SiO₂ substrate with the base vacuum of 5x10⁻⁸ mbar and lift-off process. The SEM image of the device is shown in Figure 1. The line width of the nanorings and nanowires are always equal. We varied the line width from 120 nm to 1200 nm. The Cr 5 nm/ Au 70 nm was deposited after a second level lithography followed by lift off. An a.c. current of 20 μ A is passed between the leads 1-8 (see Fig. 1) and the electrical resistance is calculated from the voltages measured simultaneously at different sections by probing different pairs of the leads. Magnetoresistance (MR) is a change in the value of the resistance of the magnetic material/devices when subjected to external magnetic field, which is applied at an angle ϕ with respect to the nano-wires.

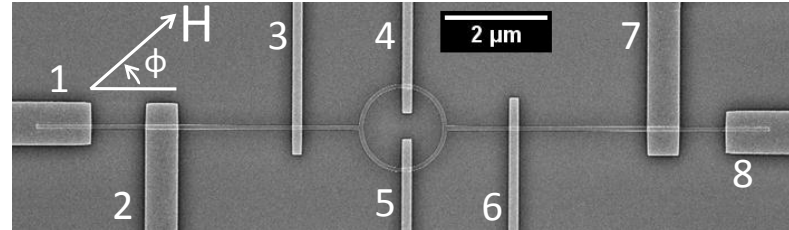


Fig.1. SEM image of the one configurations of nanoring device. The inner diameter and line width of the nanoring are 2 μ m and 120 nm respectively. The electrical contacts are labelled 1-8. Voltages V_{iy} were measured between contacts i and y for the respective resistances R_{iy} .

The MR measurements show that the devices go through various magnetic states, as the strength of the magnetic field is varied. Micromagnetic simulations performed using OOMMF (Object Oriented Micromagnetic Framework) software allows us to correlate these states to the forward-onion, vortex and reverse-onion domain configurations. The magnetic field corresponding to the switching from the vortex state to the reverse-onion state (H_{V-RO}) is highest among all the switching fields, indicating that the flux-closure state is stable. We observe a strong variation of the switching fields as a function of ϕ . H_{V-RO} measured at $\phi = 90^\circ$ is always higher than that measured at $\phi = 0^\circ$. These observations are explained by the domain wall nucleation and pinning mechanism caused by the geometry of the devices. The switching fields decreases with increasing the width of the nanoring devices due to a reduction of the demagnetization fields.

Glassy dynamics in dense assembly of active dumbbells

Rituparno Mandal,^{1,*} Pranab Jyoti Bhuyan,^{1,†} Pinaki Chaudhuri,^{2,‡} Madan Rao,^{3,4,§} and Chandan Dasgupta^{1,¶}

¹*Centre for Condensed Matter Theory, Department of Physics, Indian Institute of Science, Bangalore 560012, India*

²*The Institute of Mathematical Sciences, Chennai 600113, India*

³*Raman Research Institute, Bangalore 560080, India*

⁴*National Centre for Biological Sciences (TIFR), Bangalore 560065, India*

We study a binary mixture of self-propelled soft dumbbells at a very high density as a model *active glass-former* where a constant self-propulsion force of magnitude f_0 is introduced toward a pre-specified direction along the axis of each dumbbell in addition to thermal fluctuations. In the absence of self-propulsion this system shows dynamical arrest of both translational and rotational degrees of freedom at low enough temperatures. Through Brownian molecular dynamics simulation we investigate the effect of activity or self-propulsion in such a glass-former. A phase diagram has been drawn in the $(T - f_0)$ plane for both the degrees of freedom. We have also observed a crossover from a *thermal supercooled liquid* to an *active supercooled liquid* along an iso- τ_α^T line (where τ_α^T is the structural relaxation time for the translational degrees of freedom) on the phase diagram in the $(T - f_0)$ plane. The crossover is associated with a deviation from the Stokes-Einstein relation, formation of *vortex* like structures in the displacement fields and many other interesting features which support the fact that an *effective temperature* picture is not always adequate to explain the glass transition scenario in active matter. Our work also suggests that features like dynamical heterogeneity, cooperatively rearranging regions etc. can be qualitatively very different depending on the route of approach to the glass boundary either by reducing temperature or by reducing activity.

*Email: rituparno@physics.iisc.ernet.in

†Email: pranab@physics.iisc.ernet.in

‡Email: pinakic@imsc.res.in

§Email: madan@ncbs.res.in

¶Email: cdgupta@physics.iisc.ernet.in

Thermal conductivity of glass-forming liquids

Pranab Jyoti Bhuyan,^{1,*} Rituparno Mandal,^{1,†} Pinaki Chaudhuri,^{2,‡} Abhishek Dhar,^{3,§} and Chandan Dasgupta^{1,¶}

¹*Centre for Condensed Matter Theory, Department of Physics, Indian Institute of Science, Bangalore 560012, India*

²*The Institute of Mathematical Sciences, Chennai 600113, India*

³*International Centre for Theoretical Sciences, Bangalore 560089, India*

We present here the results of our study of heat conduction in a model glass-former through equilibrium and non-equilibrium molecular dynamics simulations. Both equilibrium and non-equilibrium simulations give similar values of thermal conductivity(κ) in a wide range of temperatures across the glass-transition. We have shown that, the thermal conductivity bears clear signature of *aging* and also the preparation procedure. These observations can be explained from the fact that the low energy inherent structures(*IS*) have low values of thermal conductivity. Further investigations within the harmonic approximation involving the density of states, participation ratio etc. seem to rationalize this feature of the inherent structures.

* Email: pranab@physics.iisc.ernet.in

† Email: rituparno@physics.iisc.ernet.in

‡ Email: pinakic@imsc.res.in

§ Email: abhishek.dhar@icts.res.in

¶ Email: cdgupta@physics.iisc.ernet.in

Spin liquid like Raman signatures in hyperkagome iridate

$\text{Na}_4\text{Ir}_3\text{O}_8$

Satyendra Nath Gupta¹, P. V. Sriluckshmy², Ashiwini Balodhi³, D. V. S. Muthu¹, S. R. Hassan², Yogesh Singh³, T. V. Ramakrishnan¹ and A. K. Sood¹

¹*Department of Physics, Indian Institute of Science, Bangalore-560012,
India* ²*The Institute of Mathematical Sciences, C.I.T. Campus, Chennai 600 113,
India* ³*Indian Institute of Science Education and Research (IISER) Mohali,
Knowledge City, Sector 81, Mohali 140306, India*

Abstract

Combining Raman scattering measurements with mean field calculations of the Raman response we show that Kitaev-like magnetic exchange is dominant in the hyperkagome iridate $\text{Na}_4\text{Ir}_3\text{O}_8$. In the measurements we observe a broad Raman band at $\sim 3500 \text{ cm}^{-1}$ with a band-width $\sim 1700 \text{ cm}^{-1}$. Calculations of the Raman response of the Kitaev-Heisenberg model on the hyperkagome lattice shows that the experimental observations are consistent with calculated Raman response where Kitaev exchange interaction (J_K) is much larger than the Heisenberg term J_1 ($J_1/J_K \sim 0.1$). A comparison with the theoretical model gives an estimate of the Kitaev exchange interaction parameter.

Reference: Phys. Rev. B 94, 155153 (2016).

Contact: satyendra707@gmail.com

A micrometre-sized heat engine operating between bacterial reservoirs

Sudeesh Krishnamurthy,¹ Subho Ghosh,² Dipankar Chatterji,²
Rajesh Ganapathy,^{3, 4} and A. K. Sood^{1, 3}

¹Department of Physics, Indian Institute of Science, Bangalore - 560012, INDIA

²Molecular Biophysics Unit, Indian Institute of Science, Bangalore - 560012, INDIA

³International Centre for Materials Science,Jawaharlal Nehru Centre for Advanced Scientific Research,Jakkur, Bangalore - 560064, INDIA

⁴Sheikh Saqr Laboratory, Jawaharlal Nehru Centre for Advanced Scientific Research,Jakkur, Bangalore - 560064, INDIA

Abstract

Artificial microscale heat engines are prototypical models to explore the mechanisms of energy transduction in a fluctuation-dominated regime^{1,2}. The heat engines realized so far on this scale have operated between thermal reservoirs, such that stochastic thermodynamics provides a precise framework for quantifying their performance^{3–6}. It remains to be seen whether these concepts readily carry over to situations where the reservoirs are out of equilibrium⁷, a scenario of particular importance to the functioning of synthetic^{8,9} and biological¹⁰ microscale engines and motors. Here, we experimentally realize a micrometre-sized active Stirling engine by periodically cycling a colloidal particle in a time-varying optical potential across bacterial baths characterized by different degrees of activity. We find that the displacement statistics of the trapped particle becomes increasingly non-Gaussian with activity and contributes substantially to the overall power output and the efficiency. Remarkably, even for engines with the same energy input, differences in non-Gaussianity of reservoir noise results in distinct performances. At high activities, the efficiency of our engines surpasses the equilibrium saturation limit of Stirling efficiency, the maximum efficiency of a Stirling engine where the ratio of cold to hot reservoir temperatures is vanishingly small. Our experiments provide fundamental insights into the functioning of micromotors and engines operating out of equilibrium.

References

1. Horowitz, J. M. & Parrando, J. M. R. A Stirling effort. *Nat. Phys.* **8**, 108–109 (2012).
2. Hanggi, P. & Marchesoni, F. Artificial Brownian motors: controlling transport on the nanoscale. *Rev. Mod. Phys.* **81**, 387–442 (2009).
3. Bickle, V. & Bechinger, C. Realization of micrometer sized stochastic heat engine. *Nat. Phys.* **8**, 143–146 (2012).
4. Martinez, I. A. *et al.* Brownian Carnot engine. *Nat. Phys.* **12**, 67–70 (2016).
5. Sekimoto, K. Langevin equation and thermodynamics. *Prog. Theor. Phys. Suppl.* **130**, 17–27 (1998).
6. Seifert, U. Stochastic thermodynamics, fluctuation theorems and molecular machines. *Rep. Prog. Phys.* **75**, 126001 (2012).
7. Das, S., Narayan, O. & Ramaswamy, S. Ratchet for energy transport between identical reservoirs. *Phys. Rev. E* **66**, 050103 (2002).
8. Browne, W. R. & Feringa, B. L. Making molecular machines work. *Nat. Nanotech.* **1**, 25–35 (2006).
9. Balzani, V. *et al.* Artificial molecular machines. *Angew. Chem. Int. Ed.* **39**, 3348–3391 (2000).
10. Howard, J. *Mechanics of Motor Proteins and the Cytoskeleton* (Sinauer Associates Sunderland, 2001).

Growth defects causing anomalous magnetic behaviour and unusual exchange bias with vertically shifted magnetic hysteresis loop in a pure antiferromagnetic system

Tanushree Sarkar

Department of Physics, Indian Institute of Science, Bangalore 560012, India

E-mail: tanushree@physics.iisc.ernet.in

Abstract for Poster

Our present antiferromagnetic system shows slight magnetic hysteresis (M-H) loop opening. In literature, there are many similar antiferromagnetic systems showing such weak ferromagnetic type behaviour. In many cases, the possible origin is assigned to either glassy interaction of ferromagnetic clusters or to spin canting without proper investigation. Our experimental findings confirm that the natural growth defects are actually causing the ferromagnetic type hysteresis. Most importantly, we see that the spins at the defect site are exchange coupled with bulk antiferromagnetic spins and few spins are pinned at the defect sites so that the field cooled M-H loops exhibit horizontal as well as vertical shift. With the vanishing of antiferromagnetic ordering above the Neel temperature (T_N), the horizontal shift of the field cooled M-H loops vanishes as usually happens in exchange-biased systems, but quite surprisingly the vertical shift persist until the loop collapses at higher temperature. This can only come from the pinned defect spins existing beyond T_N . Here, we propose a schematic model explaining possible behaviour of this defect spins resulting in horizontal and vertical shift of the M-H loops at different temperature stages. The present system being purely antiferromagnetic, without the so called ferromagnetic interaction that is generally known to be essential in realizing exchange bias property, this investigation solves many existing puzzles about the individual role of ferromagnetic and antiferromagnetic layer in an exchange bias system.

Title : Quasiparticle band structure and optical properties of hexagonal-YMnO₃

Authors : Tathagata Biswas, Manish Jain

Abstract :

We use the first principles methods to study the electronic structure and optical properties of G-type anti-ferromagnetic hexagonal-YMnO₃. Ground state properties of this material were calculated within density functional theory (DFT) using the DFT + U formalism. We calculated the quasiparticle band structure of this material using many body perturbation theory within the GW approximation. In order to understand the optical response of this material, we solved the Bethe–Salpeter equation and calculated the absorption spectrum. Our calculated optical band gap of 1.45 eV agrees well with the experimental value of 1.55 eV. We find that the exciton in this material has a interesting two dimensional localization. Our calculation show that the exciton binding energy in this material is quite large (0.21 eV). Although this large exciton binding energy would restrict it's use in most of the photovoltaic applications, the two dimensional nature of exciton in this material may open up fascinating new applications in optical nano-technology.

Origin of layer dependence in band structures of two-dimensional materials

Mit H. Naik and Manish Jain

Center for Condensed Matter Theory, Department of Physics,

Indian Institute of Science, Bangalore 560012

Abstract

We study the origin of layer dependence in band structures of two-dimensional materials. We find that the layer dependence, at the density functional theory (DFT) level, is a result of quantum confinement and the non-linearity of the exchange-correlation functional. We use this to develop an efficient scheme for performing DFT and GW calculations of multilayer systems, where multilayer properties are derived from calculations on a monolayer of the material alone. We apply this scheme to multilayers of a prototypical transition metal dichalcogenide (TMDC), MoS₂, and find excellent agreement of the derived DFT and quasiparticle band structures with the standard calculations on these. The advantage of this scheme is that it operates at a small fraction of the computation cost of a full calculation on multilayer systems, especially in the case of TMDCs where the GW calculations have very stringent convergence parameters.

Electron Phonon coupling measurement in top gated atomically thin ReS₂ transistor

Subhadip Das¹, Biswanath Chakraborty¹, Suchitra Prasad², D V S Muthu¹, Anindya Das¹, U V Waghmare² and A K Sood¹

¹Department of Physics, Indian Institute of Science, Bangalore 560012, India

²Theoretical Sciences Unit, Jawaharlal Nehru Centre for Advanced Scientific Research, Bangalore-560064, India

Abstract

Rhenium disulfide (ReS₂) is a layered semiconducting transition metal dichalcogenide (TMDC) possessing stable distorted 1T lattice structure. The reduced symmetry of these systems results in-plane asymmetry in various material properties. This leads to increased number of Raman modes than traditional 2H polytype of TMDs. Raman spectroscopy is an excellent analytical tool to probe these 2D layered materials. In-situ Raman measurement with charge carrier doping measures electron phonon coupling (EPC) strength in these systems. In this report, we systematically study the behavior of Raman modes with electron doping on atomically thin bilayer ReS₂ based field effect transistor. We report for the first time, softening and even splitting and peak broadening of some phonon modes as a function of carrier charge concentration. By measuring the variation of phonon frequency and their lifetime with doped carrier charge concentration we get an overview of the EPC in these systems.

Origin of $1/f$ Noise in MBE grown ferromagnetically doped and undoped Topological Insulators

Saurav Islam¹, Semonti Bhattacharyya¹, Abhinav Kandala^{2,3}, Anthony Richardella², Nitin Samarth², and Arindam Ghosh¹

¹Department of Physics, IISc, Bangalore 560012, India

²Department of Physics, The Pennsylvania State University, University Park, Pennsylvania 16802-6300, USA

³IBM T. J. Watson Research Center, Yorktown Heights, New York 10598, USA

Ferromagnetically doped topological insulators (FMTI) have generated enormous interest for both fundamental physics and technological applications. Addition of magnetism in TI breaks time reversal symmetry which opens a gap in surface states and leads to various interesting phenomenon such as topological magneto-electric effect and quantum anomalous hall effect. These make FMTI a suitable candidate for quantum computation and spintronics . However magnetic dopants can also lead to crystal defects and impurity band states in the insulating bulk gap. Though there have been rigorous transport and spectroscopic studies, $1/f$ noise has not been studied in these systems which is not only a key performance marker but also reveals the nature of electronic states. In this work, we have investigated $1/f$ noise in MBE grown magnetically doped Cr-(BiSb)₂Te₃ and undoped TI (BiSb)₂Te₃ as a function of chemical potential and temperature (T). In the FMTI system, the impurity induced localized states which does not have a clear signature in the average electrical transport, gives rise to a rapid increase in noise as a function of the gate voltage. In the undoped system however, there is a strong suppression of noise at the crossover from bulk to surface transport. The T dependence of noise in the FMTI sample shows peaks at certain characteristic temperatures due to generation recombination from the impurity bands whereas in the undoped, non-magnetic TI, it dependence is much weaker.

Size and layer dependence of thermally induced ripples in h-BN sheets

Indrajit Maity, Prabal K. Maiti, Manish Jain

Abstract:

Existence of long-range order in graphene has been studied using membrane theory, where the coupling between bending and stretching modes of the rippled membrane stabilize the flat phase [1, 2]. The applicability of this theory to other two-dimensional materials (one or few atoms thick) embedded in three-dimensional space has been explored both theoretically and experimentally. In this work, we simulate free standing monolayer of hexagonal Boron Nitride (h-BN) using classical molecular dynamics using Brenner-Tersoff many body potential [3]. We calculate the fourier transform of height-height correlation function ($H(q)$, where q is momentum) and find the bending rigidity by fitting $H(q)$ at small q . The bending rigidity of the monolayer (κ_{SL}) is found to be 0.83 eV. We also calculate the bending rigidity of n-layer h-BN (nh-BN) using the same methodology, where n is the number of layers of h-BN in the simulation. Our calculations show that the bending rigidity of nh-BN is larger than $n\kappa_{SL}$. We attribute the extra stiffening of the multilayer system to strong electrostatic interactions between the layers. Furthermore, we examine the stacking dependence of the bending rigidity for nh-BN.

- [1] A Fasolino, J. H. Los and M. I. Katsnelson, *Nature Materials* **6**, 858 (2007).
- [2] D. R. Nelson, T. Piran, S. Weinberg, (eds) *Statistical Mechanics of Membranes and Surfaces* (World Scientific, Singapore, 2004)
- [3] K. Albe, W. Möller, *Computational Material Science* **10**, 111-115 (1998).

Statistics of Trajectories and Geometry of Light Inertial Particles in Turbulence

P. Shubham Parashar,^{1,*} Akshay Bhatnagar,^{1,2,†} and Rahul Pandit^{1,‡}

¹*Centre for Condensed Matter Theory, Department of Physics,
Indian Institute of Science, Bangalore 560012, India.*

²*Nordita, KTH Royal Institute of Technology and Stockholm University, Roslagstullsbacken 23, 10691 Stockholm, Sweden*

Unlike Lagrangian tracers, light particles advected in fully developed turbulent flows do not follow the fluid pathlines. We investigate the trajectories these light-particles and Lagrangian tracers by looking at the time-averaged statistics of quantities like the angle ϕ between fluid velocity and particle velocity by carrying out the direct numerical simulation (DNS) of such particles in a statistically steady, homogeneous and isotropic turbulent flow. We find that under the conditions when the inertial effects of the particles can be neglected, the probability density function (PDF) of ϕ i.e. $P_\phi \sim \phi^{-4}$. We also find a non-monotonic behavior of P_ϕ with the parameter β given by $\frac{3\rho_p}{(2\rho_f + \rho_p)}$, where ρ_p and ρ_f are the densities of the particle and fluid respectively. We observe that P_ϕ is a increasing function in $\beta \in [0, 1]$, while it is a decreasing function in $\beta \in (1, 3]$. Apart from angle deviation statistics, we find that trajectory curvature κ and $\theta = |\vartheta|$ of the torsion ϑ show power-law tails for large κ and θ respectively, with exponents $h_\kappa = -5/2$ and $h_\theta = -3$; these exponents are in agreement for those previously observed for fluid pathlines and heavy particle trajectories. We propose analytical formalisms to explain the scaling laws and also find that for $\beta = 1$, $P_\phi \simeq \delta(0)$ in the limit of $t \rightarrow \infty$, a trend that we also observe in our simulations.

* pshubhamp@gmail.com

† akshayphy@gmail.com

‡ rahul@physics.iisc.ernet.in

Emergent Topological order from Spin-Orbit Density wave

Gaurav Kumar Gupta, Tanmoy Das

Department of Physics, Indian Institute of Science, Bangalore-560012

gkgupta@physics.iisc.ernet.in

Abstract

We present the theory of a new type of interaction driven Z_2 -type topological quantum order which is distinguished by the spontaneous symmetry breaking as well as a topological invariant. We show that when two oppositely polarized chiral bands [resulting from the Rashba-type spin-orbit coupling (RSOC) α_k] are significantly nested by a special wavevector $\mathbf{Q} \sim (\pi, 0)/(0, \pi)$, it induces a modulated inversion of the chirality ($\alpha_{k+Q} = \alpha_k^*$) between different lattice sites. The resulting quantum order parameter is inherently associated with a non trivial topological invariant. The corresponding quantum spin-Hall state breaks translational symmetry, but preserves time-reversal symmetry. This order parameter can be realized or engineered in two- or quasi-two-dimensional fermionic lattices, quantum wires, with tunable RSOC and correlation strength.

Electrical transport and low frequency 1/f noise study in the hybrid of molybdenum disulphide and SrTiO₃

Anindita Sahoo¹, Tathagata Paul¹, Roald Ruiter², Tamalika Banerjee², and Arindam Ghosh¹

¹Department of Physics, Indian Institute of Science, Bangalore 560 012, India

²Zernike Institute for Advanced Materials, University of Groningen, Groningen, The Netherlands

In the family of transition metal dichalcogenide, Molybdenum disulphide (MoS₂) has achieved considerable interest as a switching device in flexible electronics due to the presence of band gap leading to a high current on-off ratio. Although, the mobility of MoS₂ is quite low on usual SiO₂ substrate, it has been reported [1, 2] that in the presence of high- κ dielectric materials, MoS₂ exhibits mobility enhancement and large current on-off ratio along with very low subthreshold swing which can open up new possibilities in the practical applications of two dimensional transparent flexible electronics. In this context, SrTiO₃ (STO) is an insulating perovskite material with a very high dielectric constant ≈ 300 at room temperature. Therefore, STO may be an excellent substrate to improve the quality of MoS₂ transistor. Although, few groups have recently studied photoluminescence [3], photocatalytic effect [4] etc. in MoS₂ on STO substrate, a detailed study of electrical transport properties as well as low frequency noise has not been done yet.

In this work, we have performed a detailed electrical characterization of back gated as well as dual-gated single-layer MoS₂ field effect transistors (FET) on TiO₂-terminated (100) STO substrate. We have obtained high mobility, high current on-off ratio and low subthreshold swing in MoS₂ transistor on STO. We have also observed a strong antihysteresis in the transfer characteristics of MoS₂ depending on the back gate voltage sweep range due to that trapping of charge carriers at MoS₂-STO interface. This antihysteretic feature and the improvement of the quality of MoS₂ transistor on STO substrate may open up new possibilities in high quality memory devices based on MoS₂. Moreover, our investigation of low frequency 1/f noise indicates that trapping-detrappling of charge carriers at the MoS₂-STO interface is the dominating source of noise.

References:

- [1] Radisavljevic B., Radenovic A., Brivio J., Giacometti V. & Kis A. Single-layer MoS₂ transistors. *Nature Nanotechnology* **6** 147–150 (2011).
- [2] Perera, M. M. et al. Improved carrier mobility in few-layer MoS₂ field-effect transistors with ionic-liquid gating. *ACS Nano* **7**, 4449–4458 (2013).
- [3] Zhang, Y. et al. Dendritic, transferable, strictly monolayer MoS₂ flakes synthesized on SrTiO₃ single crystals for efficient electrocatalytic applications. *ACS Nano* **8**, 8617–8624 (2014).
- [4] Liu, J. et al. Synthesis of MoS₂/SrTiO₃ composite materials for enhanced photocatalytic activity under UV irradiation. *Journal of Materials Chemistry A* **3**, 706–712 (2015).

Multiferroic properties of hexagonal LuFeO₃ nanoparticles

Pittala Suresh and K. Vijaya Laxmi

Department of Physics, Indian Institute of Science, Bangalore – 560012, Karnataka, India

Abstract

Hexagonal LuFeO₃ nanoparticles were synthesized using the sol-gel method. XRD and neutron measurements reveals that the samples exist in single phase hexagonal structure with *P6₃cm* space group, which has polar symmetry from 6 K to 300 K. Raman spectra show 13 active phonon modes corresponding to the *P6₃cm* space group. Microstructure shows the homogeneous particles with an average grain size of 50 nm. Raman spectra show 13 active phonon modes corresponding to the *P6₃cm* space group. The Néel temperature T_N of the samples is found to be 130K. M-H loops at room temperature show paramagnetic state while it shows a canted antiferromagnetism at 3K. The magnetic structure is defined either by Γ_1 or Γ_3 configurations. The ordered site moment of Fe ions is found to be $m = 2.84 \mu_B/\text{Fe}^{3+}$ at 6 K. Room temperature ferroelectric loops are observed with remnant polarization $P_r \sim 0.18 \mu\text{C}/\text{cm}^2$ whereas Polarization measurements using PUND shows $P_r \sim 0.05 \mu\text{C}/\text{cm}^2$ confirming its structure driven multiferroicity. A clear anomaly in the heat capacity and the dielectric data is observed at the magnetic transition temperature revealing the indirect magneto-electric coupling. and the possible mechanism is explained.

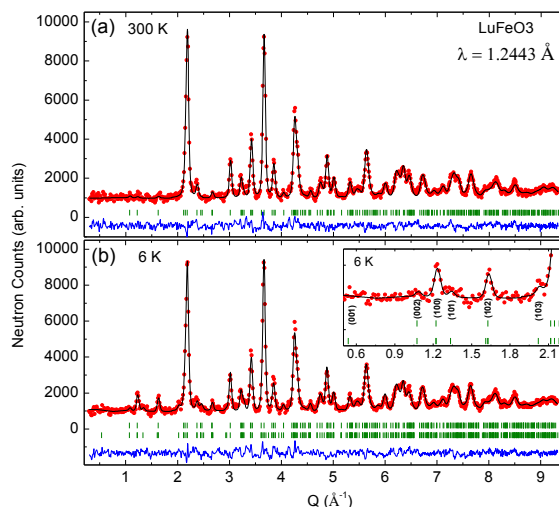


Figure 1: Experimentally observed (circles) and calculated (solid lines through the data points) neutron diffraction patterns for LuFeO₃ at (a) 300 K (paramagnetic state) and (b) 6 K (magnetically ordered state), respectively measured by PD-II ($\lambda = 1.249 \text{ \AA}$). The solid lines at the bottom of the each panel represent the difference between observed and calculated patterns. The vertical bars indicate the positions of allowed nuclear and magnetic [the bottom row in (b)] Bragg peaks. The inset of (b) shows the zoomed pattern at 6 K over the low Q -range.

Coherent mixing and control dephasing of quantum hall edge states in graphene p-n-p/n-p-n device

Chandan Kumar, Manabendra Kuiry, and Anindya Das

Department of Physics, Indian Institute of Science, Bangalore 560 012, India

We report the observation of conductance fluctuations (CFs) of graphene p-n-p/n-p-n device in quantum hall (QH) regime. We see clear evidence of CFs superimposed on the QH plateaus in the bipolar regime while in the unipolar regime flat QH plateaus are retained. CFs are shown to decrease with increasing bias and temperature. At high temperature (above 8 K) the CFs vanishes completely and the quantized plateaus are recovered in the bipolar regime. The values of QH plateaus are in agreement with the theoretical prediction based on full equilibration of chiral channels at the p-n junction. The amplitude of CFs for different filling factors follows the same trend as predicted by random matrix theory. However, there are mismatch in the values of CFs between the experiment and theory, but the amount of mismatch reduces with the increasing number of filling factors. The suppression of CFs in the experiment has been understood in terms of time dependent disorders present at the p-n junction and the role of same has been probed by low-frequency 1/f noise measurements in QH plateaus. However, the de-phasing mechanism due to the coupling between the localized states of bulk and disorder levels at the p-n junction can't be ruled out as it supports the recovery of the expected values of CFs at higher filling factors.

Abstract for poster

Accessing Rashba states in electrostatically gated topological insulator devices

Abhishek Banerjee, Ananthesh Sundaresh, Kunjalata Majhi, R Ganesan, and P S Anil Kumar

Low temperature electrical transport measurements are reported in gated BiSbTe_{1.25}Se_{1.75}/hexagonal-BN van der Waals heterostructure devices. Our experiments indicate the presence of Rashba spin-split states confined to the sample surface apart from the usual topological surface states(TSS). While previous photo-emission spectroscopy and STM experiments have observed these states, it has not been possible to unambiguously detect them by electrical means and their electrical transport properties remain largely unknown. We show that these states support high mobility conduction with Hall effect mobilities $\sim 2000 - 3000 \text{ cm}^2/\text{V-s}$ that are paradoxically much larger than the mobilities of the topological surface states $\sim 300 \text{ cm}^2/\text{V-s}$ at T=2K. The spin-split nature of these states is confirmed by magneto-resistance measurements that reveal multi-channel weak anti-localization. Our work shows that Rashba spin split states can be electrically accessed in isolation of competing electronic states in TIs. Unlike the topological surface states that have found little application despite a decade long effort, we propose that the Rashba surface states could have enormous applicability in spintronic and quantum computing technologies.

Light induced carrier transport across Van der Waals heterostructure: WSe₂- graphene

Jayanta Kumar Mishra, Avradip Pradhan, Kallol Roy and Arindam Ghosh

Van der Waals heterostructures comprising TMDc and graphene are anticipated to be a new class of materials in the field of optoelectronic and photovoltaic due to their fascinating phenomena. The appearance of the direct optical gap in the monolayer TMDC and their strong light-matter interaction make them intriguing. However, transport of carriers from one layer to another is still an obscure as it occurs through dissociation of excitons. The binding energies of excitons are reported to be around 370 meV to 790 meV in WSe₂. Neither the gate voltage nor the temperature can provide such a large binding energy. The binding energy of exciton can be reduced by dielectric screening due to different substrates to an extent, but it is still sufficiently high. Recently, Wang *et al.* theoretically proposed that exciton dissociation can be possible through an oscillating interfacial dipole by ultrafast hole transfer from one layer to another. This can be verified by looking at the behavior of different excitons (A and B) in the TMDCs. B exciton is supposed to be strongly temperature dependent as it loosely couple compared to A-exciton. To verify this experimentally, we have studied the photocurrent measurement extensively in WSe₂-graphene heterostructure. We have varied the parameters such as gate voltage, temperature, optical power, and excitation wavelengths. We have found the excitonic features (A and B) in the photocurrent spectra as well as in the relaxation time. Interestingly, B excitonic feature found to be strongly temperature dependent, which certainly proves the proposed theory. Along with that we have also able to detect the trions (charged excitons) in WSe₂.

Reference:

- 1: Wang, H. et al. Nat. Commun. 11504 (2016).

^{23}Na , ^{29}Si MAS NMR investigation of $\text{Sr}_{1-x}\text{Na}_x\text{SiO}_{3-0.5x}$ ($x=0.45$)

fast ion conductor

P. Lokeswara Rao^{*}, Bholanath Pahari[†], K. V. Ramanathan^{*}

^{*}NMR Research Center & Physics Department, Indian Institute of Science, Bangalore,
India – 560012, Mail: ^{*}kvr@sif.iisc.ernet.in

[†] Physics Department, Goa University, Taleigao Plateau, Goa, India – 403206.

A new family of ionic conductors bearing a generic formula of $\text{Sr}_{1-x}\text{Na}_x\text{SiO}_{3-0.5x}$ have generated much excitement after the recent report of very high oxide-ion (O^{2-}) conductivity [1]. Subsequent studies, based on variable temperature X-ray and neutron diffraction, electron microscopy and ^{29}Si solid state NMR have indicated that the $\text{Sr}_{1-x}\text{Na}_x\text{SiO}_{3-0.5x}$ system is two-phase material consisting of a crystalline SrSiO_3 phase with minor Na-doping and amorphous $\text{Na}_2\text{Si}_2\text{O}_5$ (AM- $\text{Na}_2\text{Si}_2\text{O}_5$) phase [2-4]. The nature of ion conduction has been reinterpreted in terms of sodium-ion (Na^+) conduction arising from AM- $\text{Na}_2\text{Si}_2\text{O}_5$ [5] phase. Here we plan to show ^{23}Na and ^{29}Si MAS NMR results in $\text{Sr}_{1-x}\text{Na}_x\text{SiO}_{3-0.5x}$ ($x=0.45$) to provide more detailed insight into the actual local environments.

References:

1. P. Singh and J. B. Goodenough, *J. Am. Chem. Soc.*, **2013**, 135, 10149.
2. I. R. Evans, J. S. OEvans, H. G. Davies, A. R. Haworth, M. L. Tate, *Chem. Mater.*, **2014**, 26, 5187.
3. C. Tealdi, L. Malavasi, I. Uda, C. Ferrara, V. Berbenni, P. Mustarelli, *Chem. Commun.*, **2014**, 50, 14732.
4. Y. Jee, X. Zhao, K. Huang, *Chem. Commun.*, **2015**, 51, 9640.
5. J. R. Peet, C. M. Widdifield, D. C. Apperley, P. Hodgkinson, M. R. Johnson, I. R. Evans, *Chem. Commun.*, **2015**, DOI: 10.1039/c5cc06644a.

Anomalous superconductivity in delta-doped semiconductors near the Mott transition

Saquib Shamim¹, Aditya Jayaraman¹, Sudhhasatta Mahapatra², Giordano Scappucci²,
Michelle Y. Simmons², Arindam Ghosh¹

¹Department of Physics, Indian Institute of Science, Bangalore – 560012, Karnataka, India

²Centre for Quantum Computation and Communication Technology, University of New South Wales, Sydney, New South Wales-2052, Australia

Abstract:

When electrons in semiconductor are confined to two dimensions, an interplay of interactions and disorder can lead to a variety of rich physical phenomena which includes metal-to-insulator transition, formation of Wigner crystal, localized magnetic moments in a non-magnetic system, quantum spin liquid, strong spin and orbital fluctuations and spontaneous breaking of time reversal symmetry. In spite of several theoretical and experimental investigations over the last few decades, the nature of ground state near the Mott transition is still debatable.

Delta-doped Si:P and Ge:P devices offer an excellent phase space to investigate the effects of strong Coulomb interactions as the strength of interaction can be tuned by varying the density of phosphorous dopants. Here, we investigate Si:P and Ge:P δ -layers contacted with superconducting (aluminium) electrodes for varying doping density of phosphorous ranging from 10^{13} cm^{-2} (near the Mott transition) to 10^{14} cm^{-2} (weakly localised metal). Temperature dependent magnetoresistance measurements show signatures of induced superconductivity when the aluminium contacts become superconducting ($T < 1\text{K}$ and $B < 10 \text{ mT}$). However, for strongly interacting devices (near the Mott transition), there exists an anomalous induced-superconducting state even beyond the critical field of Aluminium ($B \gg 10 \text{ mT}$). Nonlocal transport measurements suggest that the anomalous superconductivity could possibly arise due to long range spin fluctuations.

Non-Boltzmann thermoelectricity at a single Van der Waal junction

Phanibhusan Singhamahapatra¹, Kingshuk Sarkar¹, Subroto Mukherjee¹ and Arindam Ghosh¹

¹*Department of Physics, Indian Institute of Science, Bangalore 560 012, India.*

The recent developments of Van der Waals heterostructures made from two dimensional atomic layers have led the observation of many rich and intriguing physics in the area of thermoelectrics. For degenerate electrons, the Boltzmann formalism which relates the electronic transport coefficients to the thermoelectric coefficients, known as Mott formula, can successfully describe thermoelectric power in these low dimensional heterostructures. While Mott formula is valid in degenerate electron limit for bulk (three dimensional) materials, to low dimensional materials like graphene, nanowires and quantum dots, it remains unknown how the Boltzmann formalism unfold when the dimension of the channel approaches interatomic distance . In this work we have experimentally studied thermoelectric transport across a single Van der Waals junction formed at the overlap region of twisted bilayer graphene which is encapsulated with hexagonal Boron Nitride. At low temperature and low number density,when the electronic system is close to nondegenerate limit we observe that the measured Seebeck coefficient of the Van der Waal gap follows the Boltzmann predicted magnitude. However, if the doping or temperature is increased, when the electronic system is highly degenerate, the measured Seebeck coefficient decreases exponentially with doping density or temperature,deviating significantly from Boltzmann formalism. Our results cast a crucial insight on the role of interlayer phonon modes and electrostatic effects on thermoelectricity in interatomic limit of Van der Waal heterostructures.

Microscopic Origin of Electron Traps in Chemical Vapour Deposition grown Monolayer MoS₂ and its Grain Boundaries

Kimberly Hsieh¹, Chandra Sekhar Tiwary², Vidya Kochat², Pulickel M Ajayan² and Arindam Ghosh^{1,3}

¹ Department of Physics, Indian Institute of Science, Bangalore 560012, India

² Department of Material Science and NanoEngineering,
Rice University, Houston, Texas 77005, USA. and

³ Centre for Nano Science and Engineering, Indian Institute of Science, Bangalore 560012, India

Chemical vapour deposition (CVD) provides direct synthesis of large-area uniform domains of MoS₂ suitable for wafer-scale technologies. However, their electrical transport properties remain significantly inferior to those of mechanically exfoliated flakes due to the inevitable presence of lattice point defects and extended defects such as grain boundaries (GBs). In this work, we use electrical transport measurements to examine the physical origin of electron trap states in CVD grown MoS₂. Temperature dependence of conductance establishes variable range hopping (VRH) as the dominant transport mechanism at low temperatures (< 260 K) while electrical noise measurements exhibit McWhorter type carrier number fluctuations indicating trapping-detrapping between localised states and the channel. The density of trap states D_{it} extracted from both Mott-VRH model and McWhorter number fluctuation model clearly indicate a higher trap density for inter-grain regions ($\sim 10^{20}$ eV⁻¹ cm⁻³) than for intra-grain regions ($\sim 10^{19}$ eV⁻¹ cm⁻³) which cannot be explained solely by the oxide trap density ($\sim 10^{16} - 10^{18}$ eV⁻¹ cm⁻³). Evidently, the microscopic origin of these electron traps lie in the lattice defects within the channel rather than the oxide interface traps as previously believed.

Carrier Dynamic in Twisted Bilayer Graphene Probed by Time Resolved Terahertz Spectroscopy

Srabani Kar¹, Van Luan Nguyen², Young Hee Lee² and A. K. Sood¹

¹Department of Physics, Indian Institute of Science, Bangalore 560 012, India

²Center for Intergrated Nanostructure Physics (CINAP), Institute for Basic Science, Sungkyunkwan University, Suwon, 440-746, Korea

Abstract

We have performed transient terahertz spectroscopy to compare the photo-conductivity spectra of CVD grown Bernal stacked bilayer graphene (bBLG) and twisted bilayer graphene (tBLG) after photoexcitation. A small twisting angle present in the tBLG sample results in a gap (E_G) in band structure and corresponding joint density of states in-between the two Dirac points. Above band-gap photoexcitation results in bright resonant excitons along with the unbound free carriers. Thus we expect the response of the free carriers,to be different in twisted bilayer graphene.

We show that the photoexcited conductivity ($\Delta\sigma(\omega)$) spectra of bBLG can be described by simple Drude conductivity representing free carriers response. On the other hand $\Delta\sigma(\omega)$ of tBLG is well described by Drude-Lorentz model where the Lorentz oscillator is attributed to intra-excitonic transitions.

Log-normal electron localization in strongly gapped bilayer graphene

M. A. Aamir, Paritosh Karnatak, T. Phanindra Sai and Arindam Ghosh

The scaling theory of localization provides a seminal description of how disorder affects the electronic properties of a system. In particular, it proposes that only one parameter, the average conductance, is needed to determine the conductance distribution for all configurations of disorder layout. In 2D and 3D localized systems, the conductance distribution is normal (i.e. Gaussian) whereas in 1D, it is log-normal which means that the *logarithm* of conductance is normally distributed. In this work, we study electron localization in bilayer graphene, which is uniquely suited because of the ability to independently tune both its band gap and Fermi energy, giving a handle on the degree and regime of localization. By inducing small changes in the Fermi energy, we sample over many ensembles and obtain statistics of conductance distribution. At high densities or low electric fields, the conductance is normally distributed, as expected of the metallic regime. Remarkably, at zero number density and very high band gaps, we find the conductance distribution is *log-normal*. We note this is the first direct experimental observation of a log-normal conductance distribution. We discuss possible explanations of this result, notably of emergent 1D transport when the bulk is gapped. Furthermore, at intermediate number densities, we find a new regime of universal conductance fluctuation, possibly linked with metal-insulator transition. Our work sheds crucial experimental insights into the problem of electron localization in low dimensional systems.

Direct Measurement of Growing Interfacial Tension of Spatially Correlated Regions on Approaching the Colloidal Glass Transition

Divya Ganapathi¹, A. K. Sood^{1,2} and Rajesh Ganapathy^{2,3}

Dynamics of supercooled liquids are known to slow down dramatically close to glass transition without any obvious structural changes. Nevertheless, several theories have suggested the existence of spatially correlated structures in a glass which differ in their configurational entropy leading to interfaces with finite surface tension values. However, such interfaces have remained elusive in experimental glassy systems. Here, by characterizing amorphous arrangements in a two dimensional colloidal glassy system, we define interfaces enveloping spatially correlated regions. The fluctuations associated with these interfaces result in finite surface tension values. Our findings provide a frame work to quantify the nature and extent of spatially correlated regions around the glass transition temperature.

1)Department of Physics, Indian Institute of Science, Bangalore - 560012, India.

2) International Centre for Materials Science, Jawaharlal Nehru Centre for Advanced Scientific Research, Jakkur, Bangalore - 560064, India.

3)Sheikh Saqr Laboratory, Jawaharlal Nehru Centre for Advanced Scientific Research, Jakkur, Bangalore - 560064, India.

Title:

Experiments on atomic-scale point contacts in graphene

Authors:

AMOGH KINIKAR¹, T. PHANINDRA SAI¹, SEMONTI BHATTACHARYYA¹, ADHIP AGARWALA¹, TATHAGATA BISWAS¹, SANJOY K. SARKER², H. R. KRISHNAMURTHY¹, MANISH JAIN¹, VIJAY B. SHENOY¹ and ARINDAM GHOSH¹

¹Department of Physics, Indian Institute of Science, Bangalore 560012

²Department of Physics and Astronomy, The University of Alabama, AL 35487-0324

Abstract:

We present the observation of edge-mode transport in suspended atomic-scale constrictions of single and multilayer graphene. The constrictions were created by a novel nanomechanical exfoliation technique of graphite. Two probe conductance measurements show: quantization of conductance close to multiples of e^2/h ; split zero-bias anomaly in non-equilibrium transport; and hysteretic magneto-conductance. Atomic force microscopy of the post exfoliation sites was performed to understand the microscopic structural details of the exfoliation. It was observed that the final constriction is usually a single layer graphene with a constricting angle of 30° . Tearing along crystallographic angles suggest the tears occur along zigzag and armchair configurations with high edge fidelity. Pure edge-bound transport will be a valuable resource for room-temperature ballistic quantum circuits, spintronics and quantum information technology.

Number-resolving single photon detector from band-engineered van der Waals heterostructures

Kallol Roy, Tanweer Ahmed, Harshit Dubey, T. Phanindra Sai, Ranjit Kashid,
Shruti Maliakal, Kimberly Hsieh, Saquib Shamim, and Arindam Ghosh

Abstract: Determining the number of photons in a single optical pulse is crucial to multiple fields including single molecule spectroscopy, diffuse optical tomography, to quantum information [1, 2]. While the semiconducting transition metal dichalcogenides (TMDC) and their hybrids, are exceptional photodetectors because of their ability to absorb visible radiation down to individual molecular layers [3–8], constructing number resolving single-photon detectors (NRPD) from these two-dimensional (2D) systems has remained an outstanding technological challenge due to difficulties from low carrier mobility and large dark current noise. Here we demonstrate a NRPD device from atomically thin van der Waals hybrid of bilayer graphene (BLG) and molybdenum disulphide (MoS₂), where an electrically-induced bandgap in BLG suppresses the dark noise, while maintaining a large optoelectronic gain by separating the region of photocarrier generation (MoS₂) from the channel (BLG) of electrical transport. We achieved noise-equivalent power (*NEP*) as low as 3×10^{-22} W.Hz^{-1/2} at specific detectivity (*D**) exceeding 10^{18} cm.Hz^{1/2}.W⁻¹ (Jones) at temperatures ≈ 83 K, thus exceeding the performance of commonly used NRPDs by nearly three orders of magnitude [1, 2]. This allowed direct counting of ~ 1 to $\sim 10^5$ photons in individual optical pulses of varying power, outlining a new optoelectronic design with van der Waals heterostructures.

- [1] Rosenberg, D., Lita, A. E., Miller, A. J. & Nam, S. W. Noise-free high-efficiency photon-number-resolving detectors. *Phys. Rev. A* **71**, 061803 (2005).
- [2] Miller, A. J., Nam, S. W., Martinis, J. M. & Sergienko, A. V. Demonstration of a low-noise near-infrared photon counter with multiphoton discrimination. *Appl. Phys. Lett.* **83**, 791–793 (2003).
- [3] Koppens, F. *et al.* Photodetectors based on graphene, other two-dimensional materials and hybrid systems. *Nature Nanotech.* **9**, 780–793 (2014).
- [4] Britnell, L. *et al.* Strong light-matter interactions in heterostructures of atomically thin films. *Science* **340**, 1311–1314 (2013).
- [5] Roy, K. *et al.* Graphene-MoS₂ hybrid structures for multifunctional photoresponsive memory devices. *Nature Nanotech.* **8**, 826–830 (2013).
- [6] Zhang, W. *et al.* Ultrahigh-gain photodetectors based on atomically thin graphene-MoS₂ heterostructures. *Sci. Rep.* **4** (2014).
- [7] Massicotte, M. *et al.* Picosecond photoresponse in van der Waals heterostructures. *Nature Nanotech.* **11**, 42–46 (2016).
- [8] Roy, K. *et al.* Optically active heterostructures of graphene and ultrathin MoS₂. *Solid State Commun.* **175**, 35–42 (2013).

Transverse Thermoelectric response and Diamagnetism as a probe of superconducting fluctuation, vortex-Nernst-boundary in quasi-2D High T_c superconductors

Kingshuk Sarkar¹, Sumilan Banerjee², Subroto Mukerjee^{1,3}, T V Ramakrishnan^{1,4}

¹ Department of Physics, Indian Institute of Science, Bangalore 560 012, India

² Department of Condensed Matter Physics, Weizmann Institute of Science, Rehovot 76100, Israel

³ Centre for Quantum Information and Quantum Computing, Indian Institute of Science, Bangalore 560 012, India

⁴ Department of Physics, Banaras Hindu University, Varanasi 221005, India

Abstract. We study superconducting systems from our recently rationalized model of cuprates Phys. Rev. B **83**, 024510 (2011), Ann. Phys. **365**, (2016) in the regime where superconductivity is destroyed by superconducting fluctuations. We calculate the transverse thermoelectric co-efficient α_{xy} as a function of doping, magnetic field and temperature and find close connection with the static diamagnetic response ($-M_z$) in the fluctuation regime ranging from strong phase fluctuation dominated underdoped regime to the more conventional amplitude fluctuation dominated overdoped regime and find reasonable agreement with the experimental data and available estimates. By employing a model where pairing scale increases and superfluid density decreases with underdoping we demonstrate that 1) α_{xy} and M_z constitutes together a strong probe of superconducting fluctuations in the pseudogap phase of cuprate superconductor where the dimensionless quantity $\frac{-M_z}{\alpha_{xy}T}$ is $\mathcal{O}(1)$ and reaches a fixed value at high temperature region. 2) the transport co-effecient α_{xy} tracks the superconducting dome finding similarity with our earlier result Ann. Phys. **365**, (2016) where M_z was seen to follow the dome indicating that both these quantities are related with superfluid density scale. We discuss and analyse the boundary of the superconducting fluctuation namely the vortex-Nernst regime based on our results.

Unconventional Phases of Attractive Fermi Gases in Synthetic Hall Ribbons

Sudeep Kumar Ghosh

Department of Physics, Indian Institute of Science, Bangalore 560 012, India

A novel way to produce quantum Hall ribbons in a cold atomic system is to use M hyperfine states of atoms in a 1D optical lattice to mimic an additional “synthetic dimension”. A notable aspect here is that the $SU(M)$ symmetric interaction between atoms manifests as “infinite ranged” along the synthetic dimension. We study the many body physics of fermions with attractive interactions in this system. We use a combination of analytical field theoretic and numerical density matrix renormalization group (DMRG) methods to reveal its rich ground state phase diagram, including unconventional phases such as squished baryon fluids. Remarkably, changing the parameters entails novel crossovers and transitions, e. g., we show that increasing the magnetic field (that produces the Hall effect) may convert a “ferrometallic” state at low fields to a “squished baryon superfluid”(with algebraic pairing correlations) at high fields. We also show that this system provides a unique opportunity to study quantum phase separation in a multiflavor ultracold fermionic system.

Reference:

Phases of Attractive Fermi Gases in Synthetic Dimensions, **Ghosh, S. K.**,
Greschner, S., Yadav, U. K., Mishra, T., Rizzi, M. and Shenoy, V. B. –
[arXiv:1610.00281](https://arxiv.org/abs/1610.00281) (2016).

\mathcal{PT} -Symmetric Non-Hermitian Superconductor

Ananya Ghatak, and Tanmoy Das

Department of Physics, Indian Institute of Science, Bangalore-560012, India.

The recently developed parity and time-reversal (\mathcal{PT})-symmetric non-Hermitian (NH) systems offer a rich variety of new and characteristically distinct physical properties, which may or may not have any corresponding analog in the usual Hermitian counterparts. Encouraged by the observations of superconductivity in various dynamically driven systems where non-Hermiticity may concur, we study an unconventional, NH superconductor (NH-SC) with imaginary and odd-parity order parameter which preserves the combined \mathcal{PT} -symmetry. We construct the corresponding Bardeen-Cooper-Schrieffer (BCS) theory for such a system in the \mathcal{PT} -symmetric unbroken region where it has real energy. We obtain several characteristically distinct properties in the NH-SCs, for example, the pairing arises from repulsive interaction, the critical exponent of the gap function deviates from 1/2 (in case of H-SC) to around 1, which reflects in characteristic changes in the thermodynamic properties and in the Meissner effects. More significantly, our self-consistent BCS result, supported by the Ginzburg-Landau analysis, reveals that the NH-SC is associated with a robust first-order, discontinuous phase transition, while its Hermitian counterpart gives a second order one.